Neuroanatomical and Functional Consequences of Oxytocin Treatment at Birth

William M. Kenkel, Richard J. Ortiz, Jason R. Yee, Allison M. Perkeybile, Praveen Kulkarni, C. Sue Carter, Bruce S. Cushing, Craig F. Ferris

ABSTRACT:

Birth is a critical period for the developing brain, a time when surging hormone levels help prepare the fetal brain for the tremendous physiological changes it must accomplish upon entry into the 'extrauterine world'. A number of obstetrical conditions warrant manipulations of these hormones at the time of birth, but we know little of their possible consequences on the developing brain. One of the most notable birth signaling hormones is oxytocin, which is administered to roughly 50% of laboring women in the United States prior to / during delivery. Previously, we found evidence for behavioral, epigenetic, and neuroendocrine consequences in adult prairie vole offspring following maternal oxytocin treatment immediately prior to birth. Here, we examined the neurodevelopmental consequences in adult prairie vole offspring following maternal oxytocin treatment immediately. Control prairie voles and those exposed to 0.25 mg/kg oxytocin were scanned as adults using anatomical and functional MRI, with neuroanatomy and brain function analyzed as voxel-based morphometry and resting state functional connectivity, respectively. Overall, anatomical differences brought on by oxytocin treatment, while widespread, were generally small, while differences in functional connectivity, particularly among oxytocin-exposed males, were larger. Analyses of functional connectivity based in graph theory revealed that oxytocin-exposed males in particular showed markedly increased connectivity throughout the brain and across several parameters, including closeness and degree. These results are interpreted in the context of the organizational effects of oxytocin exposure in early life and these findings add to a growing literature on how the perinatal brain is sensitive to hormonal manipulations at birth.

BACKGROUND:

Oxytocin (OXT) is a potent and pleiotropic hormone that surges at birth to help facilitate the tremendous changes that both mammalian mothers and their offspring must accomplish upon delivery (1–3). As of 2019, 29.4% of laboring women in the U.S. received OXT to induce labor (4), and according to available survey data, this figure raises to ~50% of birthing women in America when considering OXT used to either induce and/or augment labor (5). This obstetric practice is of interest to neuroscience because there is evidence OXT can cross the placenta (6) and a growing literature suggests the neonatal brain is particularly sensitive to OXT around the time of birth, when OXT receptor (*Oxtr*) expression begins to accelerate (7) and OXT neurons in the brain undergo intense remodeling (8). Indeed, the long-term, developmental effects of OXT manipulations in early life are well-documented (9,10), which suggests the perinatal period may be a *sensitive period* with regard to the impact of OXT.

Some initial studies suggested higher rates of autism spectrum and attention deficit / hyperactivity disorder amongst children born to women whose labors were induced with OXT; however, meta-analysis of these findings suggest that any such conclusions remain premature (11). While there have been conflicting reports as to whether OXT administered to induce / augment labor is associated with increased rates of autism spectrum disorder or autistic-like behavior in offspring, considerations of dose add an important degree of nuance to this topic (12,13). Thus, regardless of whether the consequences of obstetrically administered OXT raise to the level of a neurodevelopmental disorder, the question of whether OXT affects offspring neurodevelopment is of great public health relevance given its widespread use.

Previously, we investigated the impact of maternally administered OXT on offspring neurodevelopment and behavior using the socially monogamous prairie vole (14). We found that fetal physiology was indeed sensitive to maternally administered OXT and that, in the fetal brain, such OXT dose-dependently increased methylation of the *Oxtr* promoter. In adulthood, OXT-exposed offspring of both sexes were found to demonstrate a broadly gregarious phenotype such that they exhibited more spontaneous alloparental care toward unrelated pups and spent more time in close social contact with opposite-sex adults. Male voles exposed to OXT also showed increased density of OXT receptor in the central amygdala, insular cortex, and parietal cortex, while showing decreased vasopressin receptor density in the ventral pallidum.

Because OXT is a pleiotropic hormone, we opted for a broad survey of the brain in the present study, carrying out whole-brain resting functional connectivity to further characterize the scope of the neurodevelopmental consequences of OXT exposure at birth. Here, we used magnetic resonance imaging (MRI) to scan the brains of adult male and female prairie vole offspring originally born to pregnant females treated with 0.25 mg/kg OXT on the expected day of delivery. We examined both anatomical measures (voxel based morphometry (VBM) and diffusion-weighted imaging (DWI)) as well as functional measures (resting state functional connectivity (rs-fMRI) and several graph theory measures detailed below).

METHODS:

Subjects

Prairie vole offspring (*Microtus ochrogaster*) were generated as previously described (14). All procedures were conducted in accordance with the National Institutes of Health Guide for the Care and Use of Laboratory Animals and were approved by the Institutional Animal Care and Use Committee of Northeastern University. On the expected day of delivery, pregnant females were either injected intraperitoneally with OXT (0.25 mg/kg, 'OXT') or left undisturbed ('Control'). Offspring were only included if they were delivered within 24 hours of OXT treatment. Offspring were raised by their birth parents as we previously observed no effect of maternal-OXT treatment on offspring outcomes (14). At 20 days of age, OXT and Control offspring were weaned into same-sex sibling pairs and were left to mature. Upon reaching adulthood (postnatal days 60-70), OXT and Control offspring underwent three neuroimaging scans: aT1-weighted anatomical scan for voxel based morphometry scan (VBM), an awake, resting state functional scan (rs-fMRI), and an anesthetized diffusion-weighted imaging scan (DWI), as detailed below. Subject offspring consisted of 17 Control females, 19 Control males, 17 OXT females, and 16 OXT males. From these, 7 Control females, 12 Control males, 13

OXT females and 13 OXT males were ultimately included in the rs-fMRI analyses after removing subjects due to motion artefact or technical difficulties.

Neuroimaging

All neuroimaging measures were collected using a Bruker BioSpec 7.0T/20-cm Ultra Shield Refrigerated horizontal magnet (Bruker, Billerica, MA). A 20-G/cm magnetic field gradient insert (inner diameter 12 cm) was used to scan anesthetized subjects using a quadrature transmit/receive volume coil (inner diameter 38 mm). Imaging sessions began with an anatomical scan with the following parameters: 20 slices; slice thickness, 0.70 mm; field of view, 2.5 cm; data matrix, 256 x 3 x 256; repetition time, 2.5 seconds; echo time (TE), 12.0 ms; effective TE, 48 ms; number of excitations, 2; and total acquisition time, 80 seconds.

Voxel Based Morphometry (VBM)

The following procedures were adapted for use in the vole from those described previously for rats (15). For each subject, the atlas (image size 256 x 256 x 63) (H × W × D) was warped from the standard space into the subject image space (image size 256 × 256 × 40) using the nearest-neighbor interpolation method. In the volumetric analysis, each brain region was therefore segmented, and the volume values were extracted for all 111 regions of interest (ROIs), calculated by multiplying unit volume of voxel (in mm^3) by the number of voxels using an in-house MATLAB script. To account for different brain sizes, all ROI volumes were normalized by dividing each subject's ROI volume by their total brain volume.

Diffusion-weighted Imaging (DWI)

The following procedures were identical to those described previously (16,17). Diffusion-weighted imaging (DWI) was acquired with a spin-echo echo-planar imaging (EPI) pulse sequence with the following parameters: repetition time/TE, 500/20 ms; 8 EPI segments; and 10 noncollinear gradient directions with a single b-value shell at 1000 seconds/mm^2 and 1 image with a b-value of 0 seconds/mm^2 (referred to as b0). Geometrical parameters were as follows: 48 coronal slices, each 0.313 mm thick (brain volume) and with in-plane resolution of 0.313 x 3 x 0.313 mm^2 (matrix size, 96 x 3 x 96; field of view, 30 mm^2). The imaging protocol was repeated 2 times for signal averaging. DWI acquisition took 35 to 70 minutes. DWI included diffusion-weighted three-dimensional EPI image analysis producing fractional anisotropy (FA) maps and apparent diffusion coefficient. DWI analysis was implemented with MATLAB (version 2017b) (The MathWorks, Inc., Natick, MA) and MedINRIA version 1.9.0 (http://www-sop.inria.fr/asclepios/software/MedINRIA/index.php) software.

Each brain volume was registered with the three-dimensional MRI Vole Brain Atlas template (Ekam Solutions LLC, Boston, MA) allowing voxel- and region-based statistics (18). In-house MIVA software was used for image transformations and statistical analyses. For each vole, the b0 image was coregistered with the b0 template (using a 6-parameter rigid-body transformation). The coregistration parameters were then applied on the DWI indexed maps for each index of anisotropy. Normalization was performed on the maps providing the most detailed and accurate visualization of brain structures. Normalization parameters were then applied to all indexed maps and then smoothed with a 0.3-mm Gaussian kernel. To ensure that preprocessing did not significantly affect anisotropy values, the nearest neighbor option was used following registration and normalization.

Resting State Functional MRI (rs-fMRI)

We used the same equipment and scanning protocols as in our recent work; for complete details see (18–20). Data were analyzed as 111 nodes corresponding to brain regions specified in a vole-specific atlas (18). Pearson's correlation coefficients were computed per subject across all node pairs (6105), assessing temporal correlations between brain regions. Then, r-values' (-1 to 1) normality were improved using Fisher's Z-transform. For each group, 111×111 symmetric connectivity matrices were constructed, each entry representing the strength of edge. An $|Z|=2.3$ threshold was used to avoid spurious or weak node connections (21).

Network Analyses

Graph theory network analysis was generated using Gephi, an open-source network and visualization software (22). For all groups, the absolute values of their respective symmetric connectivity matrices were imported as undirected networks and a threshold of |Z|=2.3 was applied to each node's edges to avoid spurious or weak node connections (23).

Betweenness Centrality

Betweenness centrality analyzes occurrences where a node lies in the path connecting other nodes (24). Let $\mathrm{n}_{i,j}^{\mathrm{k}}$ be the number of pathways from *i* to *j* going through *k*. Using these measures of connection, the betweeness of vertex *k* is:

$$B_k = \sum_{ij} \frac{n_{ij}^k}{n_{ij}}.$$

Degree Centrality

Degree centrality indicates the number of associations of a specific node (25). Non-weighted, binary degree is defined as:

$$C_D(j) = \sum_{j=1}^{n} A_{ij}$$

where *n* is the number of rows in the matrix in the adjacency matrix ***A*** and the elements of the matrix are given by A_{ij}, the number of edges between nodes *i* and *j*.

Closeness Centrality

Closeness centrality measures the average distance from a given starting node to all other nodes in the network (26). Closeness is defined as:

$$C(x) = \frac{N-1}{\sum_y d(y,x)}$$

where *d(y,x)* is the distance between vertices *x* and *y* and *N* is the number of nodes in the graph.

Statistics

Normality tests of control females, control males, OXT females and OXT males were performed to examine if parametric or non-parametric assumptions were required for future analysis. Shapiro-Wilk's tests were performed to examine normality assumption for degree, closeness and betweeness centrality values. Regional p-values that were greater than 0.05 were assumed to be normal. A corresponding list of nodes that classified a region is detailed in table S1. After assumptions of normality were validated, one-way ANOVA tests were used to compare differences in degree, closeness and betweenness centralities between groups. When necessary, a nonparametric Kruskal-Wallis test was performed if there was evidence against normality assumption. Statistical differences between groups were determined using a Mann-Whitney U test (a = 5%). The following formula was used to account for false discovery from multiple comparisons:

$$P(i) \leq \frac{i}{\mathrm{V}} \frac{q}{\mathrm{c(V)}}$$

P(i) is the p value based on the t test analysis. Each of 111 regions of interest (ROIs) (i) within the brain containing V ROIs. For graph theory measures, statistical analyses were calculated using GraphPad Prism version 9.0.0 for MacOS (GraphPad Software, San Diego, California USA, www.graphpad.com). For post-hoc analyses of graph theory parameters, Holm-Šídák test (for parametric) and Dunn's (for nonparametric) were used after correction for multiple comparisons.

RESULTS:

We observed a number of differences in VBM measures; however most were small to very small in effect size (Figure 1 and Tables 1-3). Within the Control group, there was only a single sex difference in regional volume; within the OXT group, however, OXT females had larger volumes in 8 of 17 cortical regions and smaller volumes in 11 brainstem / cerebellar regions compared to OXT males (Table 1). Similarly, Control males had larger volumes in 9 of 17 cortical regions and smaller volumes in 9 brainstem / cerebellar regions compared to OXT males (Table 2). Comparing within females, OXT treatment at birth resulted in smaller volumes in 4 of 17 cortical regions (Table 3). Control animals generally had larger amygdalar volumes than OXT animals (4 of 6 subregions in males; 2 of 6 in females). When morphometry data from all 111 brain regions were loaded into a PCA, the overall explanatory value of dimensions 1 and 2 was modest (29.4% and 15.9% respectively) and there were impacts of both sex and treatment on dimension 1, with male sex ($F(1,69) = 4.98$, $p = 0.029$) and OXT treatment ($F(1,69) = 16.06$, $p < 0.001$) leading to greater values (Figure 2).

We observed a broad, albeit subtle pattern of effects in OXT-exposed males in DWI measures. In terms of FA, Control animals showed small but widespread sex differences, with females having greater FA than males across brain regions, a pattern not present in OXT animals due to increased FA among OXT-exposed males (Figure 3A, Tables 2 and 3). Indeed, there were no differences in either FA or ADC between OXT males and OXT females, whereas there were 62 and 48 such regions amongst Control animals. When FA data from all 111 brain regions were loaded into a PCA, there were no effects of either sex or treatment detected (Figure 3A). In terms of ADC, Control males had greater ADC values than OXT males across 84 brain regions (Table 5). While we observed widespread ADC differences between Control males and females, we observed no sex differences in ADC in the OXT-exposed condition. The PCA for ADC revealed a main effect of OXT exposure ($F(1,65) = 5.80$, $p = 0.019$) and a trend toward an interaction between sex and treatment ($p = 0.087$). Post-hoc analysis revealed that Control males having greater dimension 1 values than both OXT males ($p = 0.026$) and OXT females ($p = 0.042$). Thus, across the brain, OXT males' ADC values more closely resembled Control females and OXT females than they did Control males.

In the analyses of functional connectivity (Figures 4-8), OXT males stood out as having a widespread pattern of greater connectivity. The vast majority of connections across all groups arose from positive correlations. Male sex and OXT treatment both increased the proportion of significant connections for both positive and negative connections (chi-square $p < 0.001$ for both effects). Whereas Control females were found to have significant functional connectivity in 5% of all possible connections, OXT females had significant connectivity in 7.2% of connections. Whereas Control males had connectivity in 6.3% of connections, OXT males had significant connectivity in 12.5% of connections (Figure 4A). Similarly, male sex and OXT treatment at birth both increased the strength of connectivity among region-region pairs whose activity was significantly correlated, but only for positively correlated pairs ($p < 0.001$ for both effects, Figure 4B). Thus, OXT led to more regions significantly functionally connected and stronger correlations in such regions among males and to a lesser extent among females (Figures 4,5). In examining the pattern of results within correlation matrices, we observed a concentration of stronger connectivity among regions of the same cluster (Figure 4D and E). This led us to examine the strength of intra- vs. inter-cluster connectivity as a function of sex and birth treatment, which revealed that male sex and OXT treatment increased intra-cluster connectivity (e.g. central amygdala and medial amygdala) to a greater degree than inter-cluster connectivity (e.g. central amygdala and dentate gyrus, Figure 4C). As shown in Figure 5, when comparing the strength of connectivity at the level of regional clusters (e.g. all subregions of the amygdala), we observed a treatment effect in the medulla and olfactory system, however there were no significant post-hoc differences. There was also two treatment by sex interactions such that OXT males had weaker connectivity than OXT females across the thalamus ($p < 0.002$) and stronger connectivity than OXT females across the cortex ($p < 0.001$).

We next examined three indices from analyses based in graph theory: betweenness, closeness, and degree (see above for definitions of each). In terms of *betweenness,* male sex and OXT treatment both increased betweenness in the basal ganglia (Figure 6, $p < 0.01$ for both effects). In terms of *closeness,* we observed similar albeit more widespread effects, with male sex and OXT treatment and both increasing closeness across several regional clusters (Figure 7). Lastly, similar effects were found in terms of *degree*, with OXT males having greater degree across a wide swath of regional clusters (Figure 8).

DISCUSSION:

Here we describe how, in prairie voles, exposure to exogenous OXT at birth can impact neurodevelopment in ways that impact neural anatomy and functioning into adulthood. Overall, anatomical differences, while widespread, were generally small, whereas differences in functional connectivity, particularly among OXT-exposed males, were larger. Anatomically, OXT at birth led to a slight reduction in amygdalar volume and OXT males in particular had slightly smaller cortices and slightly larger brainstem / cerebellums (Tables 1-3). OXT at birth led to males resembling females in terms of FA and ADC (Figure 3). However, functionally, OXT males showed marked differences from all other groups. OXT at birth led males to display robustly increased functional connectivity throughout the brain (Figures 4-8). This was particularly the case across the cortex in males in terms of the strength, closeness, and degree of connectivity (Figures 5, 7, and 8). Both the number (Figure 4A) and strength (Figure 4B) of positively correlated connections were greater in males and OXT-exposed animals. This was true both within cluster and, to a lesser extent, between clusters as well (Figure 4C). When these effects were examined regionally, few regions stood out (Figure 5); thus, we view these effects as reflecting broad, brain-wide differences. In terms of graph theoretical analyses of functional connectivity: the basal ganglia stood out for both sex and OXT increasing betweenness, whereas such differences were more widespread for closeness and degree. What does this notably broad increase in functional connectivity mean for the OXT males? We have at present only a few hints.

Interestingly, the observed effects of OXT at birth extended beyond brain regions with dense expression of the OXT receptor. The robust and widespread changes in OXT males' neural physiology (i.e. functional connectivity) were greater than the changes observed in neuroanatomy (i.e. VBM and DWI). If OXT males are continuously experiencing high levels of communication between brain regions, we would expect that to eventually produce changes in anatomical connectedness. Either our anatomical measures of connectivity were insufficiently sensitive to detect these changes, or the relatively small changes in anatomy we did detect are sufficient to produce functional changes that are comparatively more robust. The functional connectivity scans were undertaken with subjects lightly anesthetized, so it is unlikely that OXT males were responding differentially to the conditions of scanning. Furthermore, we have observed no evidence of stress reactivity being affected by perinatal OXT in our previous studies. OXT acts as a pleiotropic hormone around the time of birth to coordinate the transition from fetal to neonatal life (1), so by affecting neurodevelopmental trajectory, a single OXT exposure could produce such widespread differences across the brain.

We highlight one set of findings in particular because of their relevance to our previous work. As adults, males exposed to OXT via maternal administration at birth had denser OXT receptor distributed along the extent of the agranular insular cortex (14). In the present study, OXT treatment at birth led to the agranular insular cortex registering as a smaller volume in the brains of adult males (Table 3), along with a slight increase in FA (Table 5) and decrease in ADC (Table 8). Moreover, OXT males' agranular insular cortex had a greater number of functionally connected regions (35 vs. 19 for Control males) and stronger average connectivity among those regions (z-score 3.45 vs. 2.98 for Control males). Changes in the functioning of the agranular insular cortex correspond to the behavioral effects previously observed, such as increased alloparental caregiving (14).

One pattern generally observed in the brains of humans with autism spectrum disorders is diminished long-distance functional connectivity and increased short-distance functional connectivity (27,28). We observed that both male sex and OXT treatment at birth led to increased intra-cluster connectivity (analogous to increased short-distance hyperconnectivity), but also to increased inter-cluster connectivity, though to a lesser extent. Thus, the present results do not entirely resemble the equivalent effects seen in humans with autism spectrum disorders. While some epidemiological studies have suggested a link between autism spectrum disorders and perinatal oxytocin exposure (11), residual confounding by either genetic or environmental vulnerabilities, could explain this apparent association. Indeed, our previous work, we observed a broadly gregarious phenotype in OXT-exposed voles (14); if such results translated to humans, they would support the contention that underlying vulnerabilities bring on both a need for OXT in the mother and susceptibility to autism spectrum disorders in the child. While our previous work found behavioral differences in both males and

females exposed to OXT, which is somewhat in contrast to the present study's findings, we also found males to be much more affected by perinatal OXT in terms of neuroanatomy, which was assessed as the density of OXT and AVP receptors -and that finding matches those of the present study. Numerous previous studies have found sex- , dose-, and region-dependent effects of early life oxytocin manipulation (9,29).

There have been very few studies on the impact of birth interventions and subsequent brain development (1,3). In the realm of neuroanatomy, Deoni and colleagues recently reported that CS results in smaller brain volumes in neonatal mouse pups (30). However, no such findings have been observed in human children or infants (31). In terms of VBM and functional connectivity in the present study, OXT led males toward a more masculinized phenotype. In terms of ADC and FA, however, OXT led males toward a more feminized phenotype. Further work is needed to reveal the meanings of these differences.

This study is not without limitations. Firstly, because the Control group did not receive a vehicle treatment, the effects of injection were not adequately controlled for, which introduced a stress confound of indeterminate magnitude. In a small validation study, adult offspring of saline-treated dams (n = 3 female, 5 male adult offspring) were not found to have meaningful differences in DWI values compared to the un-treated Control animals of the present study (n = 17 female, 19 male adult offspring).

Collectively, these results support the contention that the perinatal brain is sensitive to OXT administered indirectly to the pregnant female. As obstetric care continues to use OXT for labor induction / augmentation in the majority of births in the U.S. (4,5), a more complete understanding of the neurodevelopmental effects of OXT exposure at delivery is imperative. Furthermore, as delayed cord clamping becomes standard practice (32), this will extend both the duration and dose of potential OXT exposure by the neonate, since the vast majority of deliveries now use OXT during the third stage of labor to prevent postpartum hemorrhage (33,34). Because the perinatal period is a sensitive period for brain development in terms of OXT exposure, these practices deserve further investigation.

Table Legends:

Table 1. A) a list of the single brain area, reticular nucleus of the thalamus, that significantly differs (p=0.021, critical value p<0.05) in volume between adult female and male voles that were treated with saline vehicle within 24 hrs of parturition. Shown are the average and standard deviation in volume in mm3 and effects size (omega square ωSq). With a false discovery rate (FDR) p=0.0017 this singular finding can be dismissed concluding there is no sex difference in brain volumes between female and male voles resulting from this early manipulation. In contrast, Table 1B lists the brain areas that are significantly different in volume between adult female and male voles exposed to OXT during birth (FDR p=0.043). The brain areas are ranked in order of significance and are truncated from a larger list of 116 areas taken from the vole MRI atlas (see Supplementary Table S1).

Table 2. The list of brain regions that were significantly different in volume between OXT females and Control females. OXT females showed smaller brain volumes in 15/21 of the affected regions (FDR p=0.036). The regions affected spread across the olfactory system (anterior olfactory nuc., piriform cortex), hypothalamus (paraventricular, anterior), amygdala (basal, extended), thalamus (anterior, paraventricular) and basal ganglia (nuc. accumbens, caudate putamen).

Table 3. The list of brain regions that were significantly different in volume between OXT males and Control males (FDR p=0.06). Males were most affected by OXT a birth showing 35/116 brain regions with significant differences from vehicle controls. As in the case of the females exposed to OXT at birth, the majority of the affected brain regions in OXT males were smaller than vehicle controls. The regions most sensitive were many of the same for females e.g. olfactory system, limbic cortex, basal ganglia, striatum, amygdala, and hypothalamus. The brain regions that were significantly larger in volume with OXT exposure were in the cerebellum (5th, 7th,8th, 9th lobules) and brainstem (gigantocellularis, trigeminal complex, cuneate nuc., medullary reticular nuc. pontine nuc.).

Table 4. The list of brain regions that were significantly different in fractional anisotropy between OXT females and Control females.

Table 5. The list of brain regions that were significantly different in fractional anisotropy (FA) between OXT males and Control males. While widespread, differences were generally small in effect, with OXT males generally showing greater FA scores.

Table 6. The list of brain regions that were significantly different in fractional anisotropy (FA) between Control females and Control males. While widespread, differences outside of the thalamus were generally small in effect, with females generally showing greater FA scores.

Table 7. The list of brain regions that were significantly different in apparent diffusion coefficient (ADC) between Control females and Control males. While widespread, differences were generally small in effect, with males generally showing greater ADC scores.

Table 8. The list of brain regions that were significantly different in apparent diffusion coefficient (ADC) between OXT males and Control males. While widespread, differences were generally small in effect, with Control males generally showing greater ADC scores. Note: there were no regions where OXT females and Control females differed in terms of ADC.

Figure Legends:

Figure 1. A 3D color coded reconstructions summarizing the significantly different brain areas with volumetric changes for each experimental condition. Details of these differences can be found in tables 1-3.

Figure 2. (A) Voxel-based morphometry (VBM) measures from 111 brain regions were loaded into a principal component analysis. The overall explanatory value of dimensions 1 and 2 was 29.4% and 15.9%, respectively. (B) Both male sex and OXT treatment lead to greater values in dimension 1 ($p < 0.029$ for both comparisons). Post-hoc analyses revealed OXT males had significantly greater dimension 1 scores than Control males (* $p = 0.017$), while OXT females tended to be greater than Control females (# $p = 0.079$). (C) There were no effects in dimension 2.

Figure 3. Diffusion-weighted imaging (DWI) measures for fractional anisotropy (FA, panels A and B) and apparent diffusion coefficient (ADC, panels C and D) from 111 brain regions were loaded into a principal component analysis. (B) There were no significant differences in FA. (D) Control males had greater dimension 1 scores than OXT males (* $p = 0.026$) and OXT females (* $p = 0.042$). in terms of ADC.

Figure 4. Resting-state functional connectivity from 111 brain regions. (A) Both OXT treatment and male sex increased functional connectivity, meaning OXT males had the greatest proportion of region-region pairs significantly functionally connected for both positive (dark fill) and negative (light fill) correlations. Significant group differences are indicated with different letters over top the bars. (B) The average strength of correlation among region-region pairs whose activity was significantly correlated. Both OXT treatment and male sex increased the strength of connectivity for positive connections (dark fill). There were no significant differences among negative connections (light fill). (C) Both OXT treatment and male sex increased the strength of connectivity among both intra- and inter-cluster, though intra-cluster connectivity was more sensitive to these effects. Significant group differences are indicated with different letters over top the bars. In panels (D) and (E), connectivity from males and females respectively, 111x111 cell matrices show the strength of connectivity for all possible pairs of brain regions. Reflected across the diagonal are opposing treatment conditions, with OXT on top and Control on bottom. Region-region pairs whose connectivity Z score was less than |2.3| were excluded.

Figure 5. A map of the strength of connectivity (i.e. correlations' z-scores) averaged over regional clusters by group. For example, the 'Hippocampus' cluster includes the: CA1, CA3, Dentate gyrus, Subiculum and Parasubiculum. * $p < 0.05$, ** $p < 0.01$, *** $p < 0.001$.

Figure 6. A map of betweenness averaged over regional clusters by group. For example, the 'Hippocampus' cluster includes the: CA1, CA3, Dentate gyrus, Subiculum and Parasubiculum. * $p < 0.0332$, ** $p < 0.0021$, *** $p < 0.0002$, **** $p < 0.0001$.

Figure 7. A map of closeness averaged over regional clusters by group. Both OXT treatment and male sex increased closeness throughout the brain, with effects most apparent in OXT males. * $p < 0.0332$, ** $p < 0.0021$, *** $p < 0.0002$, **** $p < 0.0001$.

Figure 8. A map of degree averaged over regional clusters by group. Both OXT treatment and male sex increased closeness throughout the brain, with effects most apparent in OXT males. * $p < 0.0332$, ** $p < 0.0021$, *** $p < 0.0002$, **** $p < 0.0001$.

Supplementary Figure Legends:

Table S1. The list of brain regions and their corresponding regional cluster to which they were classified.

Figure S1. The changes in brain volumes between sexes are not consistent, i.e. in some brain areas females are greater (black sign) and others less than males (red sign). The location of these different brain areas affected by OT at birth when comparing females and males can be seen in the probability heat maps in Fig 1. Brain regions that are greater in volume in females than males are organized around the olfactory system (A. glomerular layer; B. anterior olfactory n; B-D. piriform cortices) and prefrontal/limbic cortical areas (B. motor, insular; C. anterior cingulate; D. retrosplenial). Areas that are larger in males vs females are primarily associated with brainstem/cerebellum (E. reticulotegmental n., raphe, pontine reticular n; F. olivary n.; G. vestibular n., gigantocellularis, paraflocculus, F. cuneate n. 7th lobule, medullary reticular n.).

REFERENCES:

1. Kenkel, W. M., Yee, J. R. & Carter, C. S. Is oxytocin a maternal-foetal signalling molecule at birth? Implications for development. *Journal of neuroendocrinology* **26,** 739–49 (2014).
2. Kingsbury, M. A. & Bilbo, S. D. The inflammatory event of birth: How oxytocin signaling may guide the development of the brain and gastrointestinal system. *Front.Neuroendocrinol.* **55,** 100794 (2019).
3. Kenkel, W. Birth signalling hormones and the developmental consequences of caesarean delivery. *Journal of Neuroendocrinology* **n/a,** e12912 (2020).
4. Martin, J. A., Hamilton, B. E., Osterman, M. J. K. & Driscoll, A. K. Births: Final Data for 2019. *Natl Vital Stat Rep* **70,** 1–51 (2021).
5. Declercq, E. R., Sakala, C., Corry, M. P., Applebaum, S. & Herrlich, A. Major Survey Findings of Listening to MothersSM III: Pregnancy and Birth. *J Perinat Educ* **23,** 9–16 (2014).
6. Malek, A., Blann, E. & Mattison, D. R. Human placental transport of oxytocin. *J.Matern.Fetal.* **5,** 245–255 (1996).
7. Rokicki, J. *et al.* Oxytocin receptor expression patterns in the human brain across development. Preprint at https://doi.org/10.31219/osf.io/j3b5d (2021)
8. Madrigal, M. P. & Jurado, S. Specification of oxytocinergic and vasopressinergic circuits in the developing mouse brain. *Commun Biol* **4,** 1–16 (2021).
9. Hammock, E. A. D. Developmental Perspectives on Oxytocin and Vasopressin. *Neuropsychopharmacology* **40,** 24–42 (2015).
10. Bales, K. L. & Perkeybile, A. M. Developmental experiences and the oxytocin receptor system. *Horm.Behav.* **61,** 313–319 (2012).
11. Lønfeldt, N. N., Verhulst, F. C., Strandberg-Larsen, K., Plessen, K. J. & Lebowitz, E. R. Assessing risk of neurodevelopmental disorders after birth with oxytocin: a systematic review and meta-analysis. *Psychological Medicine* **49,** 881–890 (2019).
12. Guastella, A. J. *et al.* Does perinatal exposure to exogenous oxytocin influence child behavioural problems and autistic-like behaviours to 20 years of age? *J.Child Psychol.Psychiatry* **2018/04/28,** (2018).
13. Soltys, S. M. *et al.* An association of intrapartum synthetic oxytocin dosing and the odds of developing autism. *Autism* **24,** 1400–1410 (2020).

14. Kenkel, W. *et al.* Behavioral and epigenetic consequences of oxytocin treatment at birth. *Science Advances* **5,** eaav2244 (2019).
15. Lawson, C. M., Rentrup, K. F. G., Cai, X., Kulkarni, P. P. & Ferris, C. F. Using multimodal MRI to investigate alterations in brain structure and function in the BBZDR/Wor rat model of type 2 diabetes. *Animal Models and Experimental Medicine* **3,** 285–294 (2020).
16. Kulkarni, P. *et al.* Characterizing the human APOE epsilon 4 knock-in transgene in female and male rats with multimodal magnetic resonance imaging. *Brain Research* **1747,** 147030 (2020).
17. Ferris, C. F. *et al.* Alterations in brain neurocircuitry following treatment with the chemotherapeutic agent paclitaxel in rats. *Neurobiology of Pain* **6,** 100034 (2019).
18. Yee, J. R. *et al.* BOLD fMRI in awake prairie voles: A platform for translational social and affective neuroscience. *Neuroimage* **138,** 221–232 (2016).
19. Ortiz, J. J., Portillo, W., Paredes, R. G., Young, L. J. & Alcauter, S. Resting state brain networks in the prairie vole. *Scientific Reports* **8,** (2018).
20. Ortiz, R. *et al.* Differences in Diffusion-Weighted Imaging and Resting-State Functional Connectivity Between Two Culturally Distinct Populations of Prairie Vole. *Biological Psychiatry: Cognitive Neuroscience and Neuroimaging* (2020). doi:10.1016/j.bpsc.2020.08.014
21. Worsley, K. J. in *Functional Magnetic Resonance Imaging* (Oxford University Press, 2001). doi:10.1093/acprof:oso/9780192630711.003.0014
22. Bastian, M., Heymann, S. & Jacomy, M. Gephi: An Open Source Software for Exploring and Manipulating Networks. *Proceedings of the International AAAI Conference on Web and Social Media* **3,** 361–362 (2009).
23. Worsley, K. J., Evans, A. C., Marrett, S. & Neelin, P. A Three-Dimensional Statistical Analysis for CBF Activation Studies in Human Brain. *J Cereb Blood Flow Metab* **12,** 900–918 (1992).
24. Freeman, L. C. A Set of Measures of Centrality Based on Betweenness. *Sociometry* **40,** 35–41 (1977).
25. Freeman, L. C. Centrality in social networks conceptual clarification. *Social Networks* **1,** 215–239 (1978).
26. Sabidussi, G. The centrality index of a graph. *Psychometrika* **31,** 581–603 (1966).
27. Rane, P. *et al.* Connectivity in Autism: A Review of MRI Connectivity Studies. *Harv.Rev.Psychiatry* **23,** 223–244 (2015).

28. O'Reilly, C., Lewis, J. D. & Elsabbagh, M. Is functional brain connectivity atypical in autism? A systematic review of EEG and MEG studies. *PLoS ONE* **12,** (2017).

29. Carter, C. S. Developmental consequences of oxytocin. *Physiol Behav* **79,** 383–97 (2003).

30. Chiesa, M., Rabiei, H., Riffault, B., Ferrari, D. C. & Ben-Ari, Y. Brain Volumes in Mice are Smaller at Birth After Term or Preterm Cesarean Section Delivery. *Cereb Cortex* (2021). doi:10.1093/cercor/bhab033

31. Deoni, S. C. *et al.* PMC6330134; Cesarean Delivery Impacts Infant Brain Development. *AJNR Am.J.Neuroradiol.* **40,** 169–177 (2019).

32. Committee Opinion No. 684 Summary: Delayed Umbilical Cord Clamping After Birth. *Obstetrics & Gynecology* **129,** 232–233 (2017).

33. Salati, J. A., Leathersich, S. J., Williams, M. J., Cuthbert, A. & Tolosa, J. E. Prophylactic oxytocin for the third stage of labour to prevent postpartum haemorrhage. *Cochrane Database of Systematic Reviews* (2019). doi:10.1002/14651858.CD001808.pub3

34. Miranda, J. E. *et al.* The effect of guideline variations on the implementation of active management of the third stage of labor. *Int.J.Gynaecol.Obstet.* **2013/03/27,** (2013).

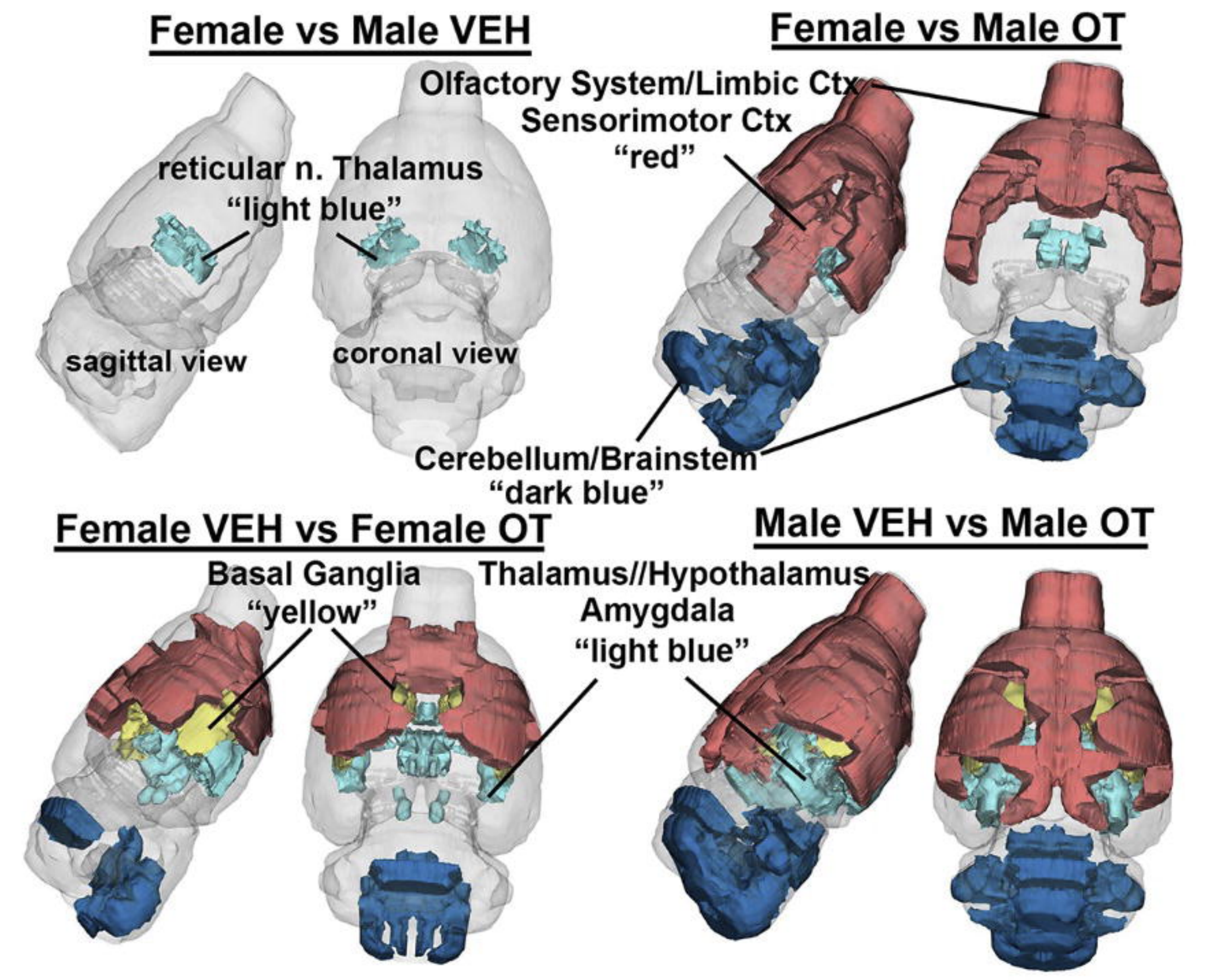
Female vs Male VEH
Female vs Male OT
Olfactory System/Limbic Ctx
Sensorimotor Ctx
"red"
reticular n. Thalamus
"light blue"
sagittal view
coronal view
Cerebellum/Brainstem
"dark blue"
Female VEH vs Female OT
Male VEH vs Male OT
Basal Ganglia
"yellow"
Thalamus//Hypothalamus
Amygdala
"light blue"

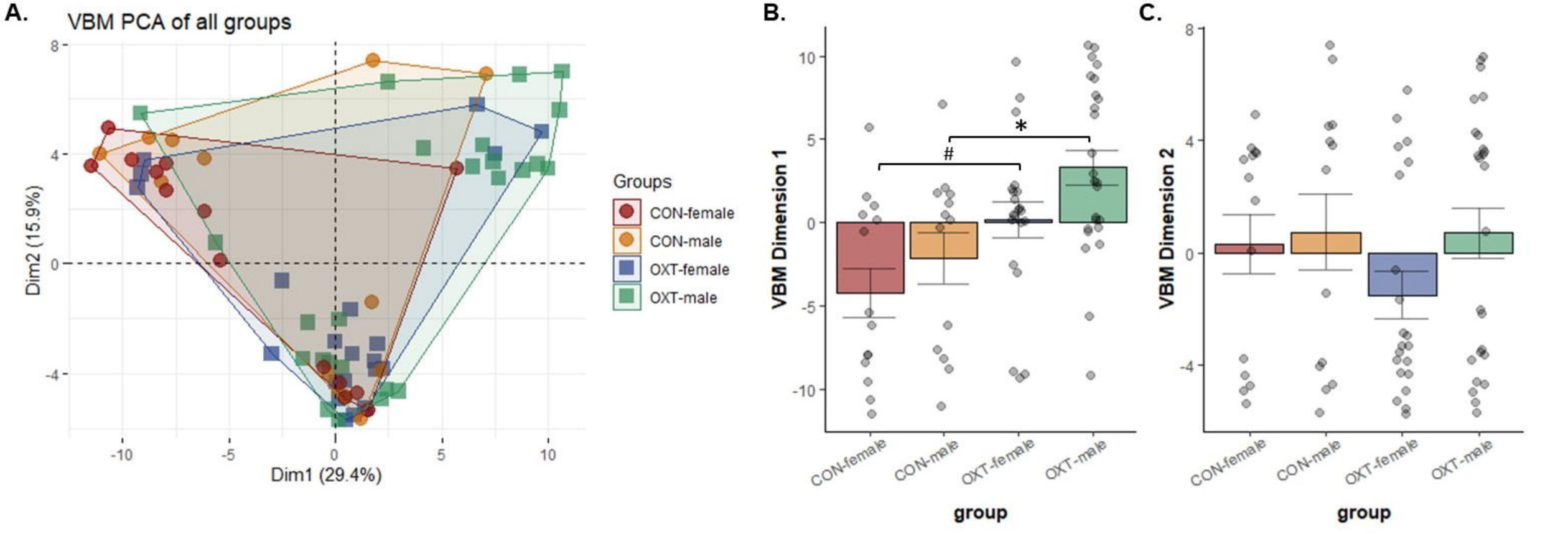
A.
VBM PCA of all groups
Dim2 (15.9%)
Dim1 (29.4%)
Groups
CON-female
CON-male
OXT-female
OXT-male
B.
VBM Dimension 1
group
#
*
C.
VBM Dimension 2
group

A.

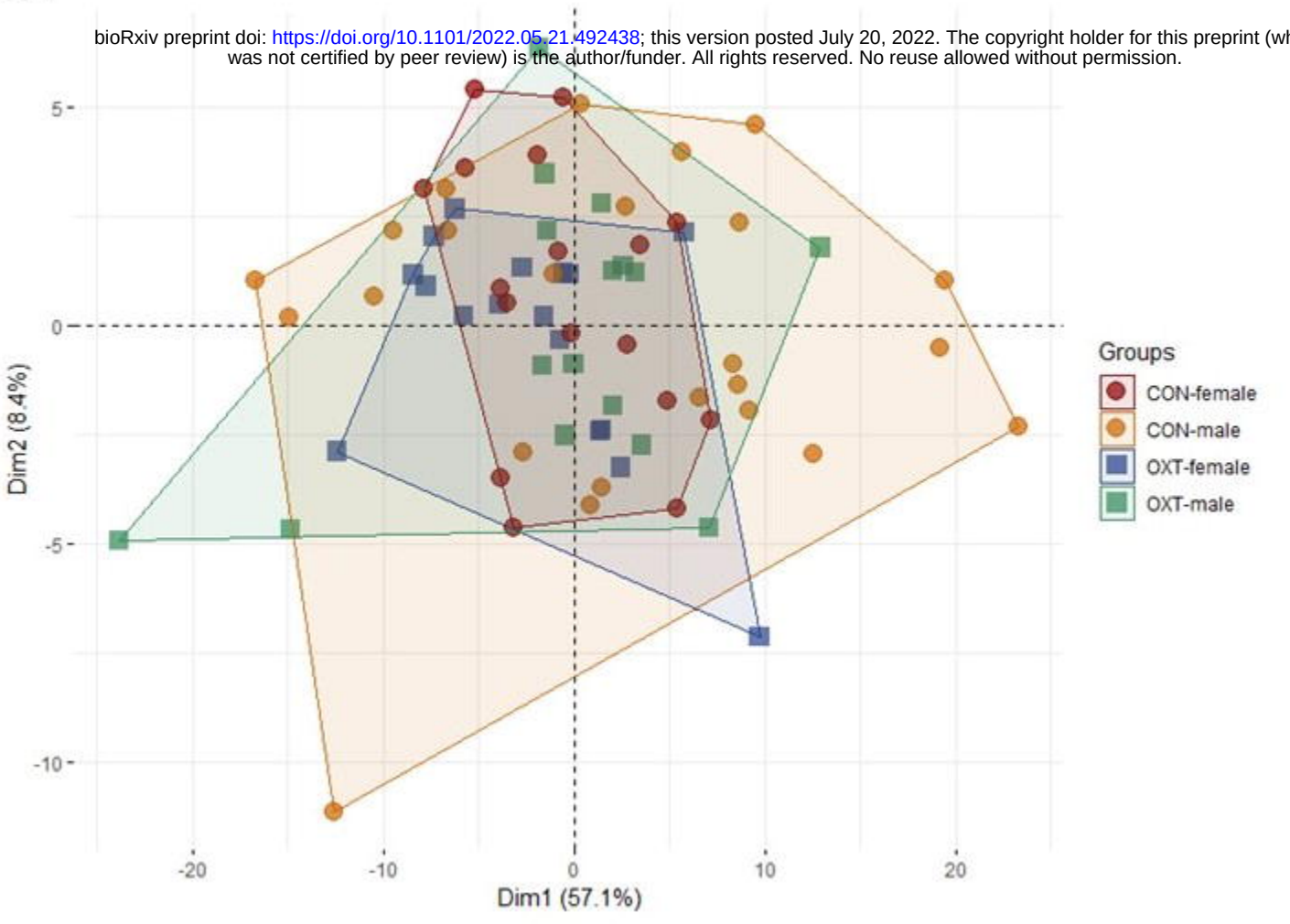

B.

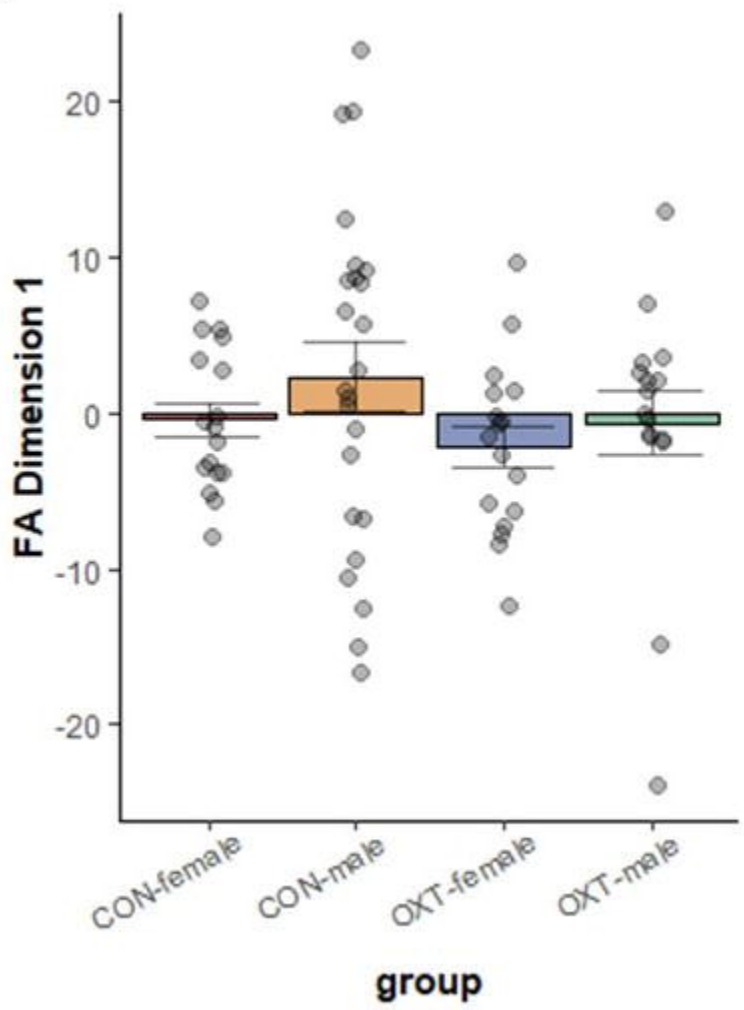

C.

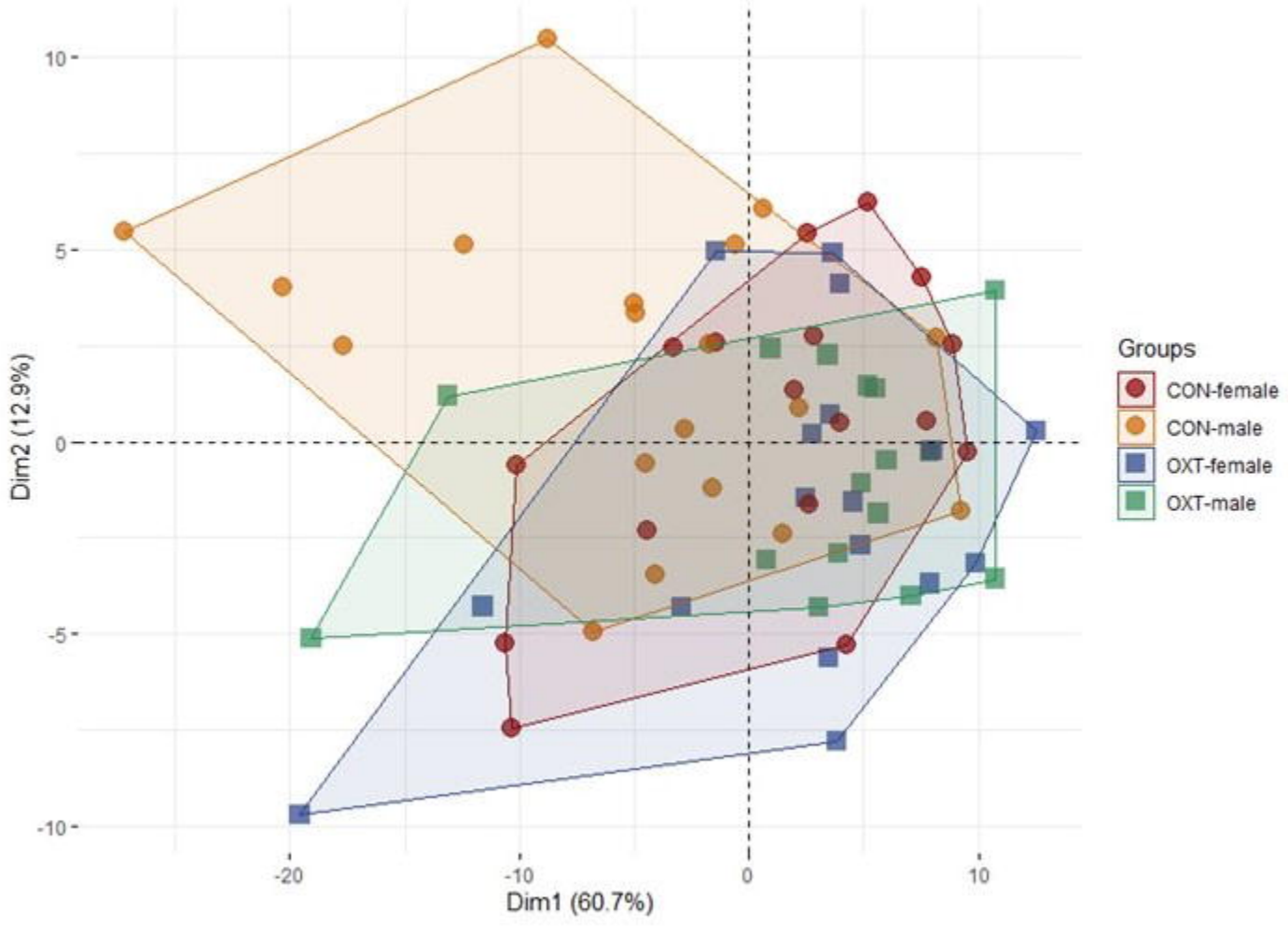

D.

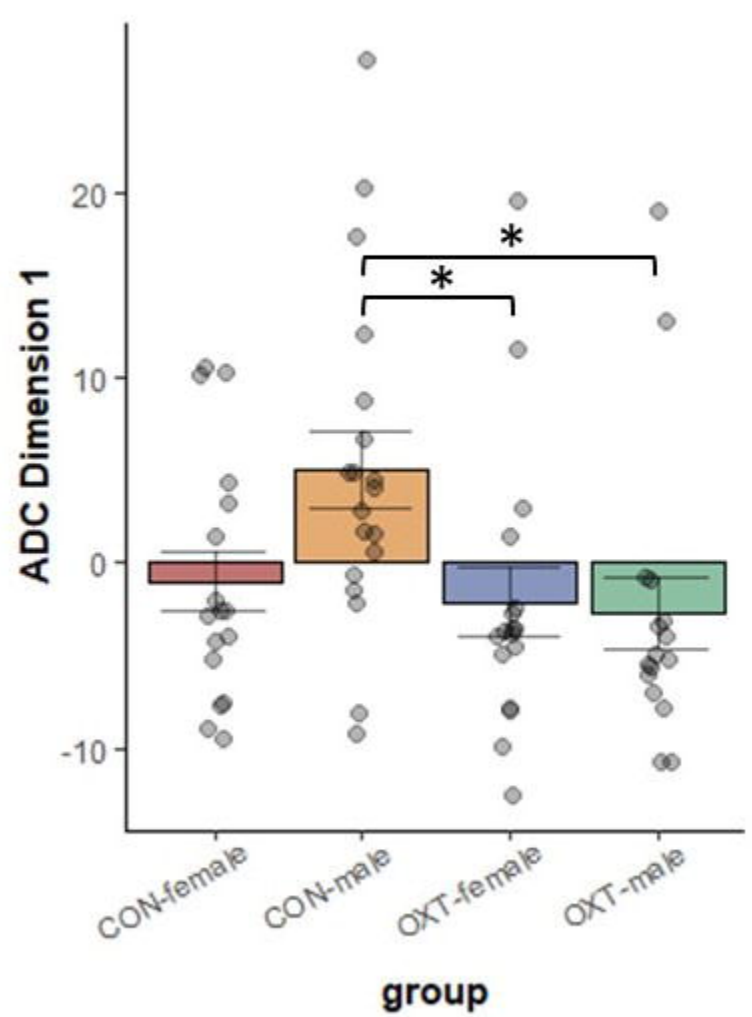

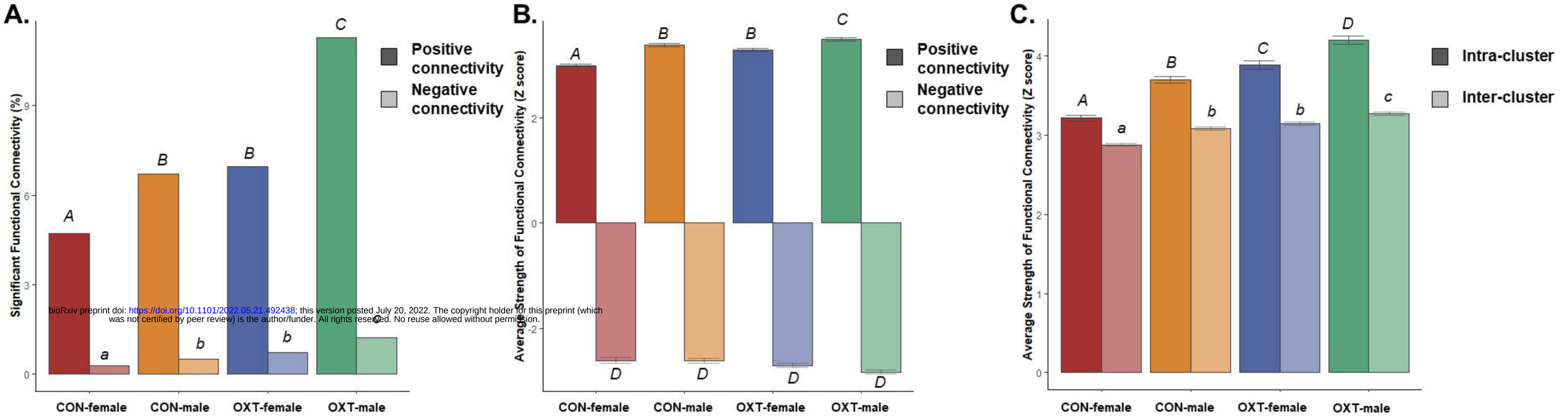

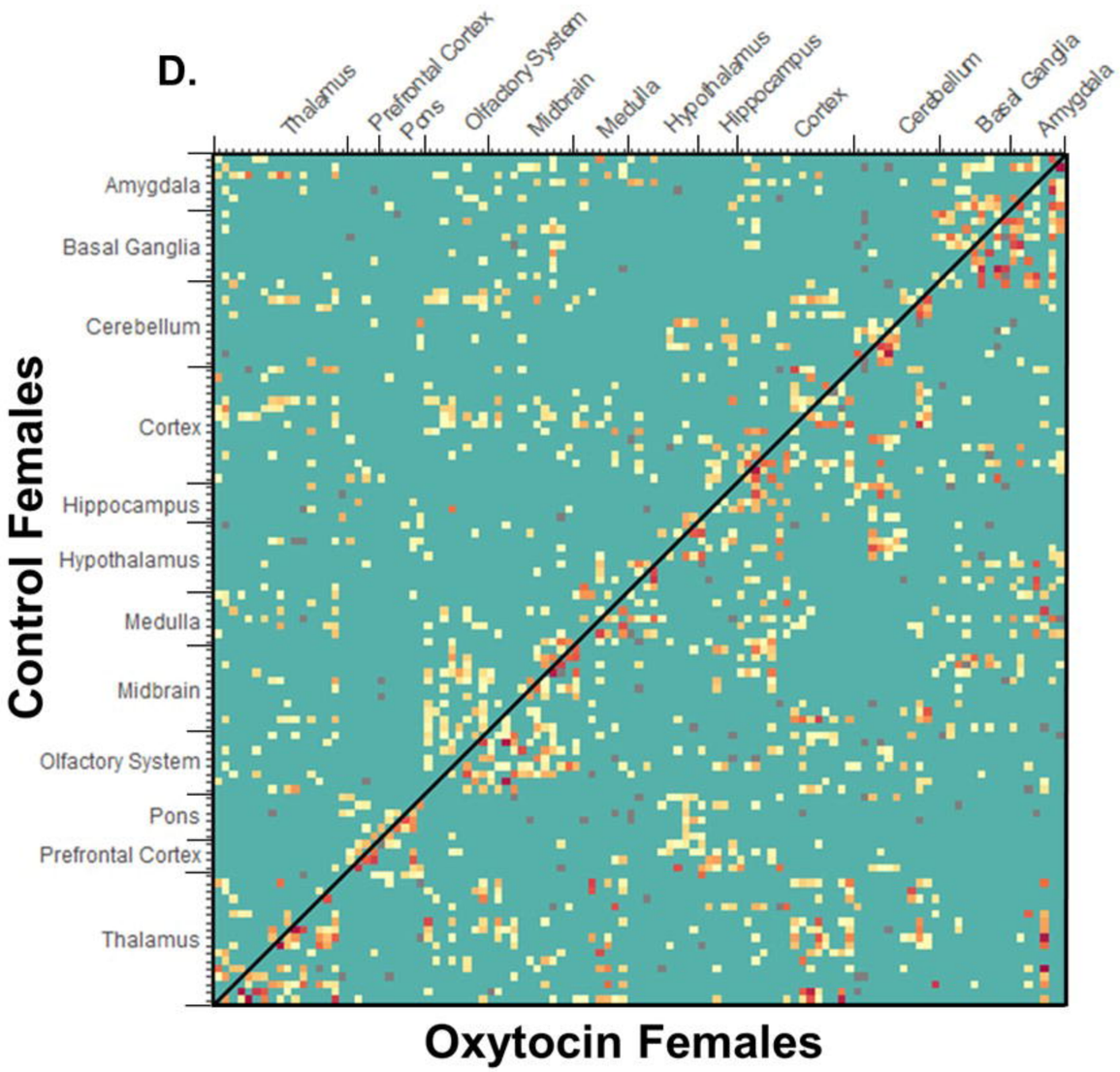

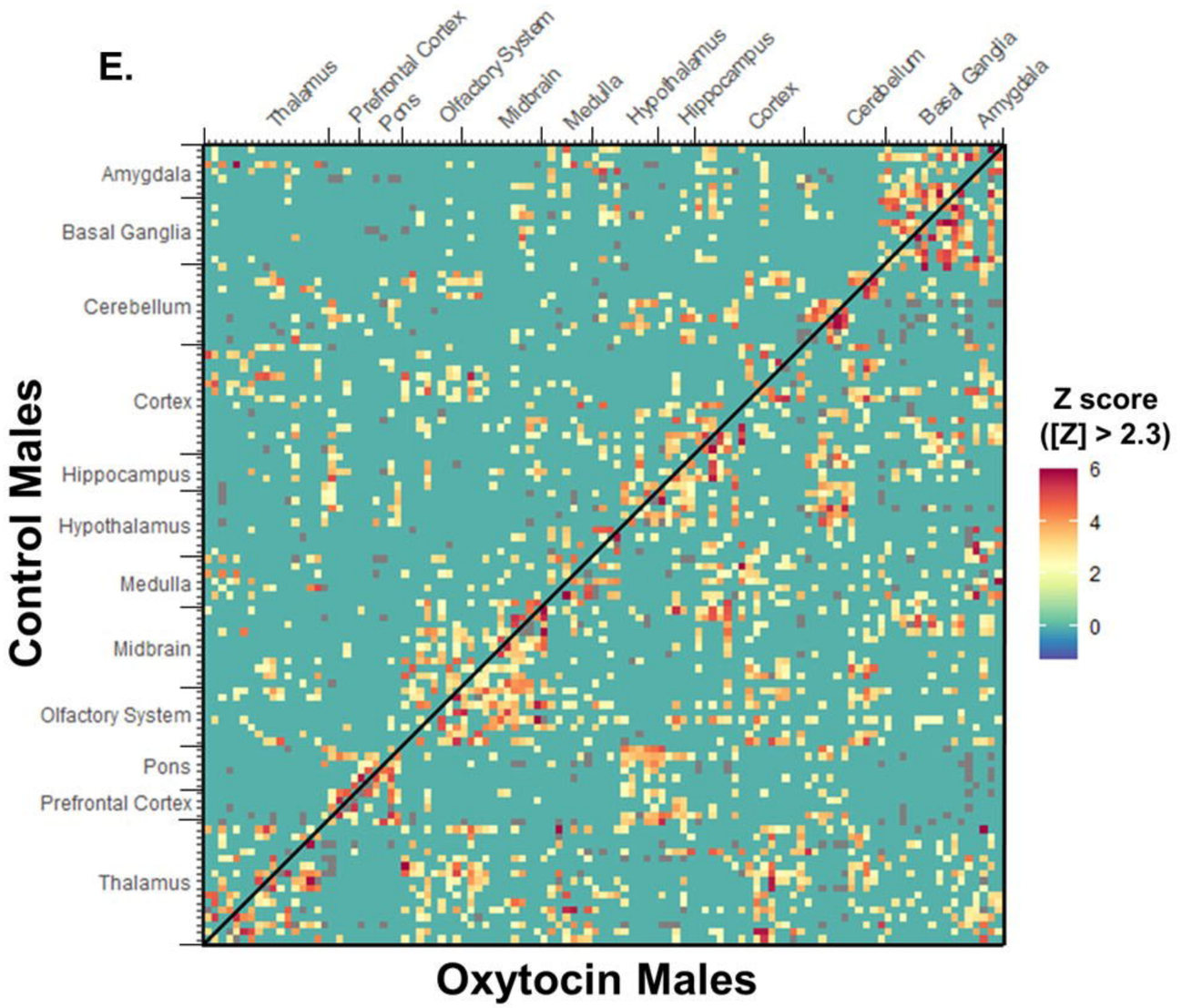

Strength of Connectivity

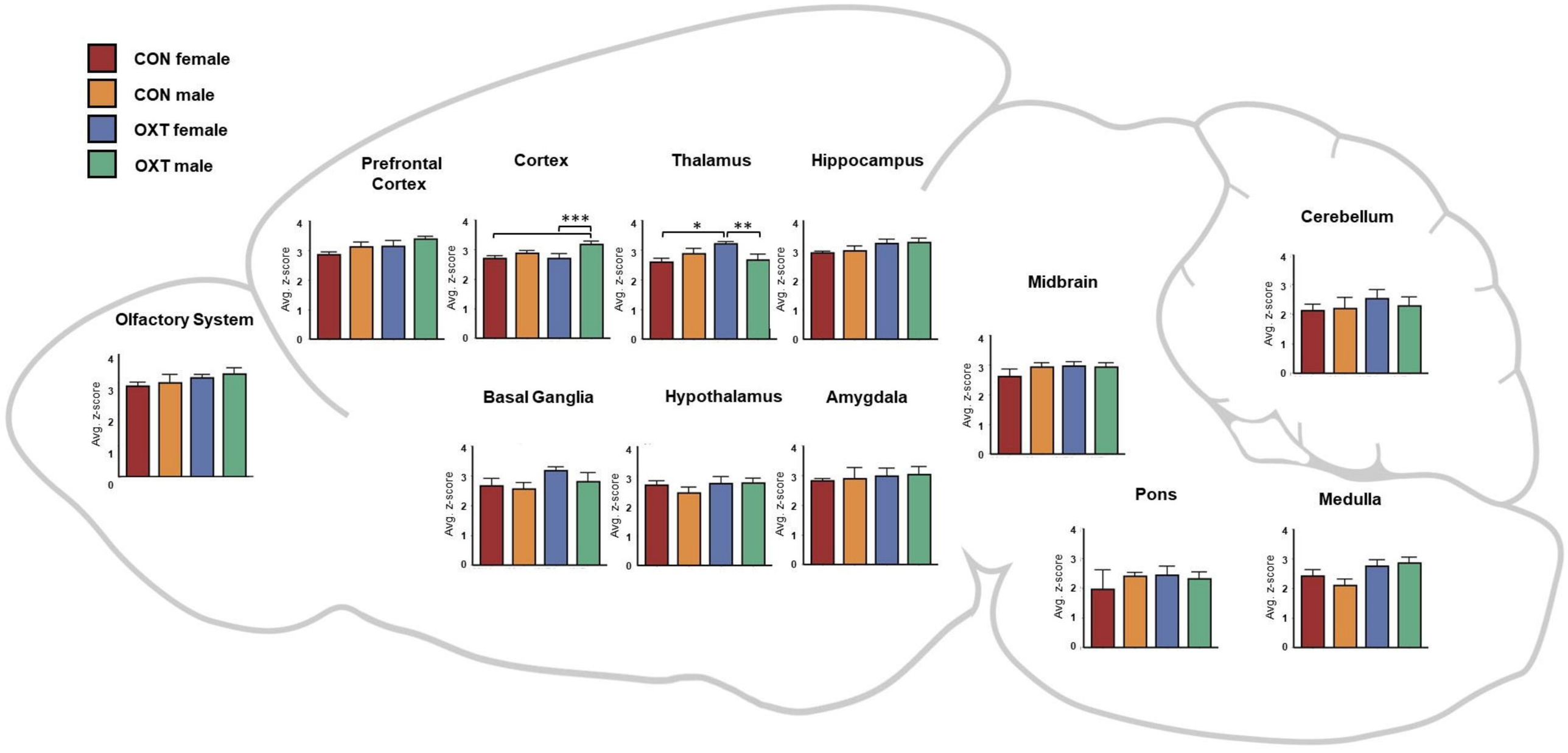

Betweenness

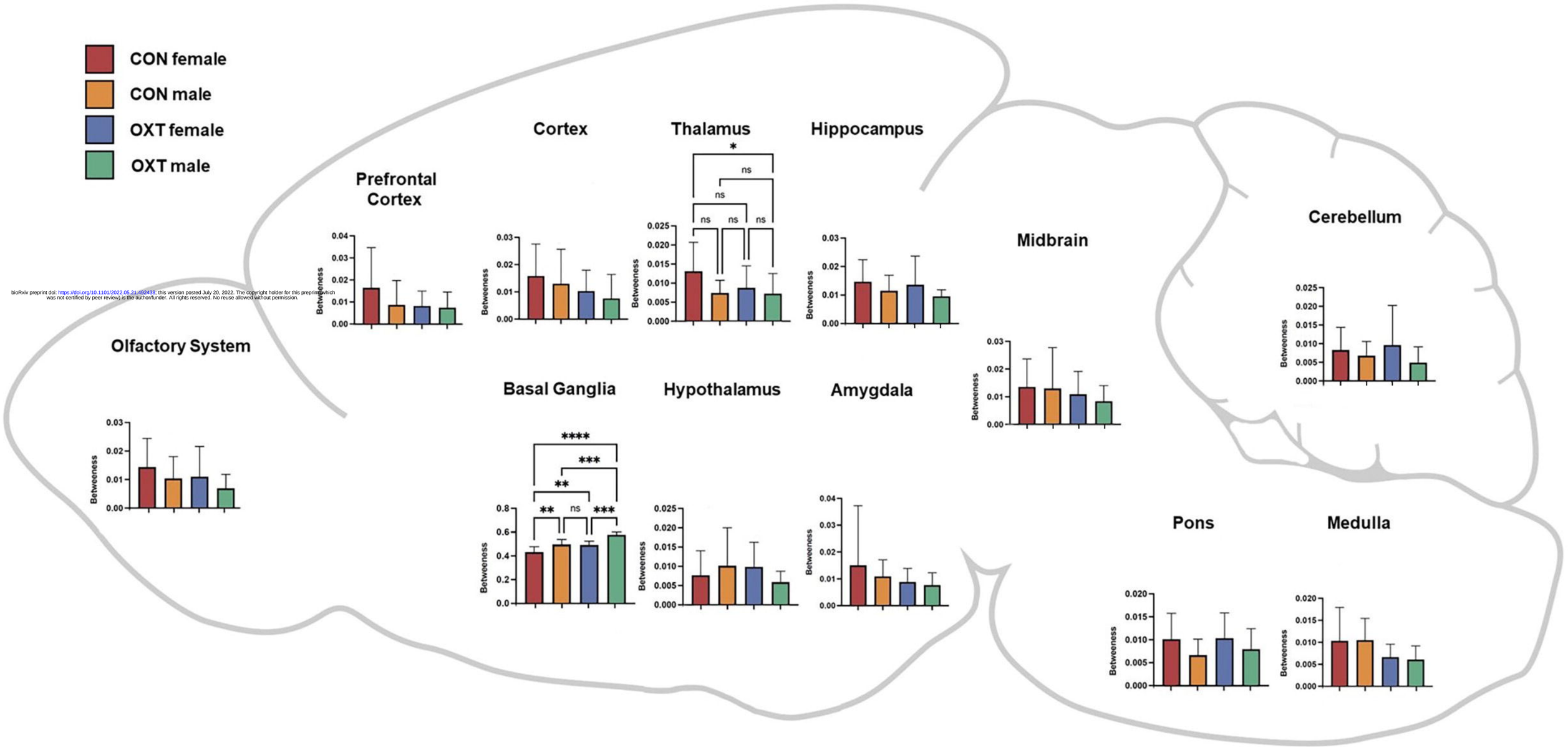

Closeness

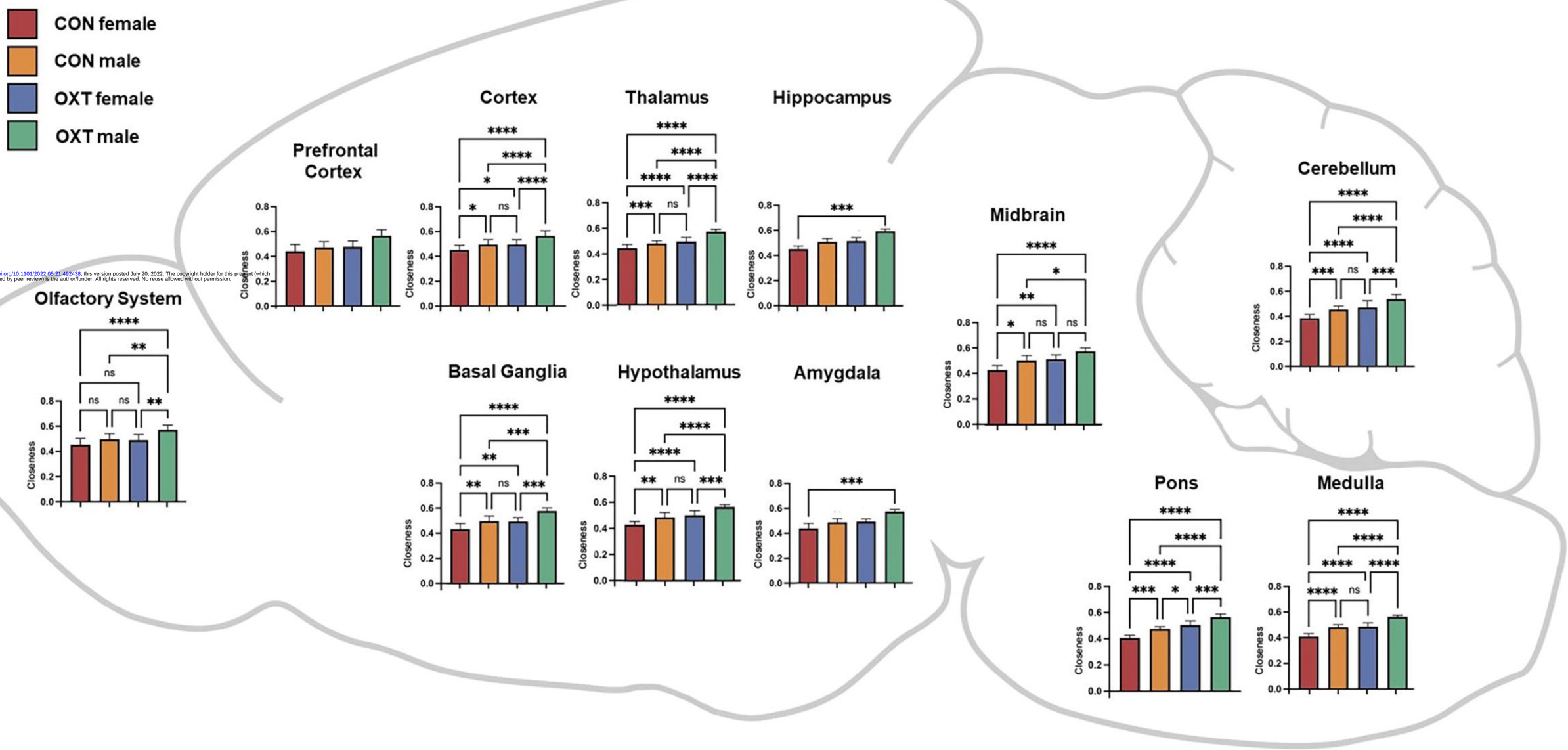

Degree

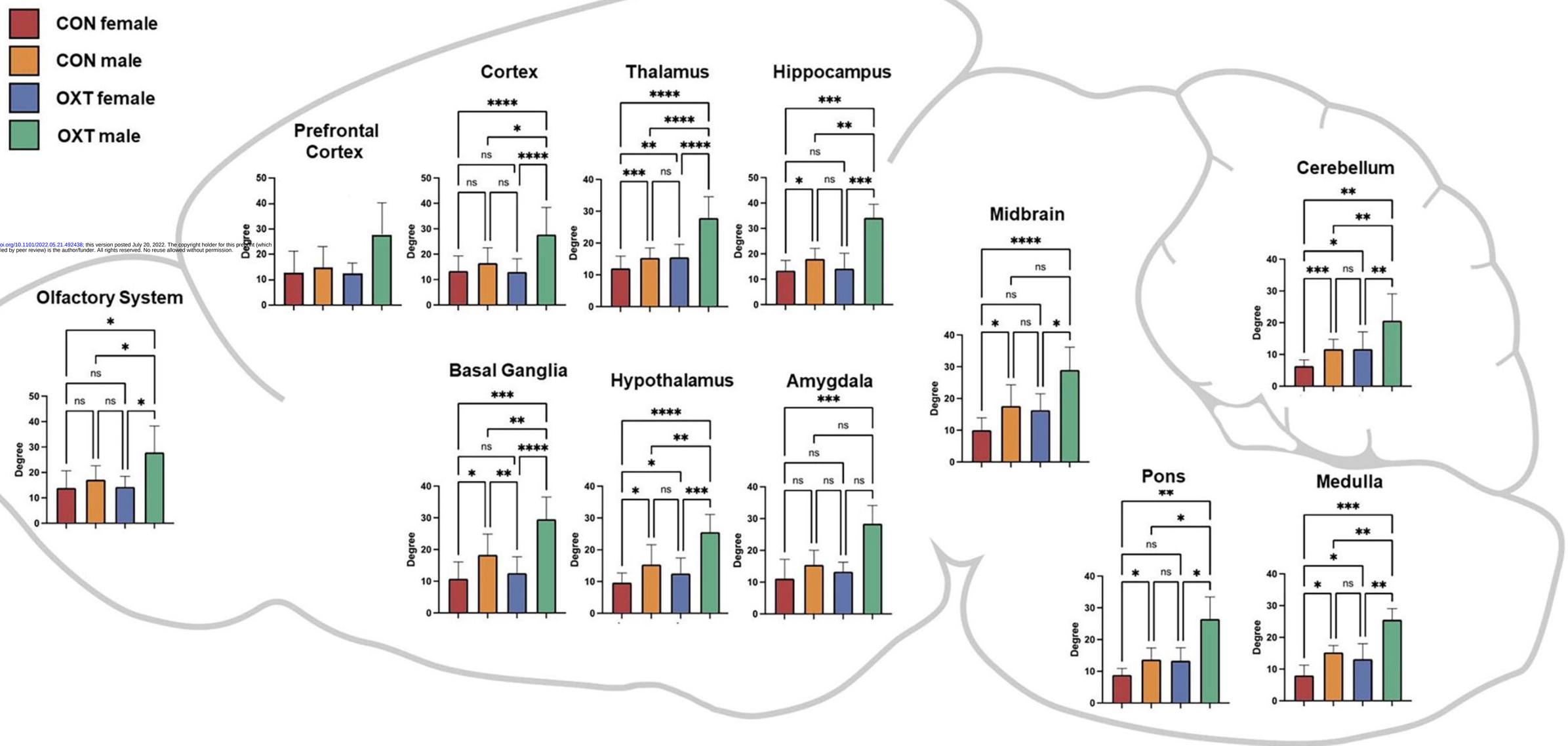

A

Female Vehicle vs Male Vehicle - Brain Volumes (mm3)							
	Female			Male			
Brain Area	Ave	SD		Ave	SD	P-val	ω Sq
reticular n.	2.6	0.4	>	2.3	0.3	0.021	0.16733

B

Female Oxytocin vs Male Oxytocin - Brain Volumes (mm3)							
	Female			Male			
Brain Area	Ave	SD		Ave	SD	P-val	ω Sq
frontal association ctx	12.4	3.1	>	9.7	2.8	0.003	0.16823
ventral tegmental area	0.6	0.2	<	0.8	0.3	0.008	0.1341
vestibular n.	1.5	0.6	<	2.2	0.8	0.009	0.12879
agranular insular ctx	11.6	2.7	>	9.7	2.5	0.010	0.12744
retrosplenial ctx	7.5	0.8	>	6.7	1.0	0.014	0.11251
gigantocellular reticular n.	5.1	1.3	<	5.8	1.6	0.017	0.10415
median raphe n.	0.5	0.2	<	0.8	0.4	0.019	0.10093
secondary motor ctx	13.1	2.2	>	11.4	2.5	0.019	0.10065
anterior hypothalamus	3.6	0.9	>	3.1	1.0	0.019	0.09949
parasubiculum	1.4	0.4	<	1.8	0.5	0.021	0.09613
paraflocculus cerebellum	5.4	1.7	<	6.1	1.6	0.022	0.09494
cuneate n.	0.1	0.2	<	0.4	0.5	0.026	0.08752
parietal ctx	2.5	0.7	>	2.1	0.6	0.029	0.08393
7th cerebellar lobule	0.6	1.4	<	2.3	2.8	0.031	0.08128
claustrum	1.9	0.5	>	1.5	0.6	0.031	0.08077
medullary reticular n.	0.9	2.2	<	2.7	3.4	0.036	0.07577
olivary n.	1.1	0.6	<	1.5	0.7	0.036	0.07557
rostral piriform ctx	11.9	1.7	>	10.5	2.3	0.039	0.07242
reticulotegmental n.	1.9	0.7	<	2.3	0.6	0.041	0.07042
pontine reticular n. oral	2.0	0.8	<	2.7	1.2	0.042	0.06945
anterior olfactory n.	14.1	2.1	>	12.2	2.8	0.045	0.06742
anterior cingulate ctx	4.1	1.1	>	3.5	0.8	0.045	0.06742
glomerular layer olfactory bulb	16.6	2.9	>	15.2	2.9	0.046	0.06642
lateral preoptic area	1.4	0.3	>	1.2	0.4	0.052	0.06168
caudal piriform ctx	9.0	1.4	>	8.3	1.2	0.052	0.0616

Female Vehicle vs Female Oxytocin - Brain Volumes (mm3)							
	Female Veh			Female OT			
Brain Area	Ave	SD		Ave	SD	P-val	ω Sq
tegmental n.	1.3	0.3	>	0.9	0.3	0.000	0.34584
paraventricular hypothalamus	0.7	0.2	>	0.4	0.2	0.001	0.28447
anterior thalamus	2.2	0.7	>	1.5	0.5	0.005	0.20755
anterior hypothalamus	4.5	0.9	>	3.6	0.9	0.007	0.18794
accumbens shell	4.5	1.5	>	3.3	1.0	0.009	0.17454
caudate putamen (striatum)	25.7	4.1	>	22.2	3.4	0.010	0.16929
solitary tract n.	0.2	0.3	<	0.5	0.4	0.012	0.1573
5th cerebellar lobule	2.3	2.5	<	4.8	2.3	0.015	0.14453
basal amygdala	5.7	0.8	>	4.9	0.8	0.016	0.14185
anterior olfactory n.	16.4	2.9	>	14.1	2.1	0.019	0.13233
paraventricular thalamus	1.2	0.3	>	1.0	0.3	0.022	0.12559
rostral piriform ctx	14.2	2.9	>	11.9	1.7	0.025	0.11863
extended amydala	2.4	1.0	>	1.8	0.6	0.026	0.11651
orbital ctx	17.7	5.9	>	12.6	3.9	0.026	0.11634
trigeminal complex medulla	2.6	1.8	<	4.1	1.7	0.035	0.10135
primary motor ctx	13.3	2.6	>	11.4	1.9	0.035	0.10126
vestibular n.	2.0	0.8	>	1.5	0.6	0.037	0.09922
diagonal band of Broca	0.4	0.3	<	0.6	0.3	0.038	0.09732
red n.	0.5	0.2	<	0.7	0.2	0.047	0.08738
primary somatosensory ctx	26.0	3.0	>	24.1	3.3	0.047	0.08697
habenula n.	0.5	0.2	<	0.7	0.2	0.049	0.08528

Male Vehicle vs Male Oxytocin - Brain Volumes (mm3)							
	Male Veh			Male OT			
Brain Area	Ave	SD		Ave	SD	P-val	ω Sq
frontal association ctx	13.4	1.9	>	9.7	2.8	0.000	0.32943
agranular insular ctx	13.6	3.8	>	9.7	2.5	0.002	0.22789
claustrum	2.4	1.0	>	1.5	0.6	0.003	0.21273
rostral piriform ctx	13.2	2.4	>	10.5	2.3	0.003	0.20768
anterior olfactory n.	14.9	1.8	>	12.2	2.8	0.004	0.1931
5th cerebellar lobule	2.7	2.8	<	5.4	2.1	0.005	0.19098
endopiriform n.	4.6	1.4	>	3.5	0.8	0.006	0.17671
primary somatosensory ctx	25.4	3.3	>	22.1	3.2	0.006	0.17439
7th cerebellar lobule	0.3	0.9	<	2.3	2.8	0.007	0.17291
accumbens core	2.3	0.7	>	1.7	0.5	0.007	0.16991
granular cell layer olfactory bulb	11.4	3.5	>	9.0	1.2	0.008	0.16111
orbital ctx	15.7	6.0	>	11.0	2.8	0.011	0.14783
globus pallidus	3.5	0.6	>	2.8	0.6	0.012	0.14374
caudate putamen (striatum)	25.0	4.6	>	21.3	3.7	0.012	0.14359
glomerular layer olfactory bulb	18.9	4.9	>	15.2	2.9	0.013	0.13943
cortical amygdala	3.5	0.5	>	3.0	0.6	0.016	0.12943
retrosplenial ctx	7.6	1.1	>	6.7	1.0	0.016	0.12923
9th cerebellar lobule	0.1	0.4	<	1.4	1.9	0.018	0.12523
cuneate n.	0.0	0.1	<	0.4	0.5	0.018	0.12523
trigeminal complex	3.1	2.6	<	4.5	1.5	0.019	0.12132
secondary somatosensory ctx	6.2	1.0	>	5.2	1.0	0.019	0.1213
visual 2 ctx	9.0	1.0	>	8.1	1.4	0.020	0.11941
zona incerta	1.6	0.2	<	1.8	0.3	0.022	0.11573
dentate gyrus	8.1	0.4	>	7.5	1.1	0.022	0.11556
basal amygdala	5.2	0.7	>	4.5	0.9	0.025	0.10986
anterior cingulate ctx	4.2	0.9	>	3.5	0.8	0.026	0.10789
caudal piriform ctx	9.3	1.1	>	8.3	1.2	0.027	0.10603
anterior thalamus	2.0	0.8	>	1.3	0.4	0.029	0.10239
gigantocellular reticular n.	4.2	2.4	<	5.8	1.6	0.031	0.09872
central amygdaloid n.	2.3	0.3	>	2.0	0.5	0.032	0.09704
anterior hypothalamic area	3.9	1.3	>	3.1	1.0	0.034	0.09515
medullary reticular n.	0.7	2.5	<	2.7	3.4	0.038	0.08917
8th cerebellar lobule	0.3	1.1	<	1.6	1.9	0.039	0.08829
pontine n.	0.5	0.2	<	0.6	0.2	0.047	0.07992
infralimbic ctx	1.0	0.3	>	0.7	0.5	0.047	0.0797

Fractional Anisotropy: Control Females vs Oxytocin Females						
Brain Area	Female Control		Female Oxytocin			
	Mean	SD	Mean	SD	P val	Effect
3rd cerebellar lobule	0.4825	0.0609	0.5259	0.0582	0.0235	*0.11782*
5th cerebellar lobule	0.489	0.0585	0.5273	0.0573	0.0388	*0.10367*
anterior cingulate ctx	0.478	0.0515	0.5141	0.0609	0.044	*0.10039*
inferior colliculus	0.4405	0.0436	0.4718	0.0561	0.0492	*0.09499*
auditory ctx	0.4565	0.0437	0.4886	0.0457	0.025	*0.09415*

Fractional Anisotropy: Control Males vs Oxytocin Males							
Brain Area	Males Control			Males Oxytocin			
	Mean	SD		Mean	SD	P val	Effect
medial preoptic area	0.47	0.06	<	0.52	0.06	0.004	0.1249
pontine nuclei	0.50	0.07	<	0.53	0.04	0.001	0.09148
medial geniculate	0.55	0.06	<	0.59	0.05	0.024	0.07966
median raphe nucleus	0.52	0.05	<	0.56	0.06	0.015	0.07972
lateral geniculate	0.52	0.06	<	0.56	0.05	0.009	0.08229
parabrachial nucleus	0.51	0.03	<	0.53	0.05	0.012	0.05862
lateral dorsal thalamic nucleus	0.50	0.06	<	0.53	0.05	0.005	0.079
reticular formation	0.52	0.05	<	0.54	0.05	0.002	0.0676
lemniscal nucleus	0.55	0.03	<	0.57	0.04	0.002	0.04745
anterior olfactory nucleus	0.48	0.07	<	0.51	0.03	0.023	0.07136
3rd cerebellar lobule	0.51	0.04	<	0.53	0.04	0.001	0.04758
ventral pallidum	0.46	0.04	<	0.49	0.06	0.026	0.07166
ventral medial nucleus	0.56	0.05	>	0.53	0.05	0.015	0.06245
reuniens nucleus	0.48	0.05	<	0.51	0.05	0.043	0.06446
trigeminal complex pons	0.51	0.06	<	0.53	0.06	0.007	0.06633
agranular insular ctx	0.55	0.06	<	0.57	0.04	0.014	0.05201
cortical amygdaloid nucleus	0.52	0.06	<	0.54	0.05	0.037	0.05807
auditory ctx	0.49	0.04	<	0.51	0.04	0.049	0.04631
medial amygdaloid nucleus	0.47	0.06	>	0.44	0.08	0.032	0.08558
periaqueductal gray	0.51	0.06	<	0.53	0.06	0.023	0.05655
ventral thalamic nuclei	0.50	0.05	<	0.53	0.07	0.027	0.05859
2nd cerebellar lobule	0.47	0.05	<	0.50	0.08	0.005	0.06362
posterior thalamic nucleus	0.52	0.06	<	0.54	0.04	0.006	0.04344
paraventricular nucleus, hypothalamus	0.48	0.06	<	0.50	0.07	0.009	0.05594
superior colliculus	0.45	0.04	<	0.46	0.06	0.012	0.05009
reticulotegmental nucleus	0.53	0.05	<	0.54	0.04	0.009	0.03172
frontal association ctx	0.53	0.05	<	0.55	0.05	0.049	0.0364
prelimbic ctx	0.53	0.05	<	0.54	0.04	0.047	0.02827
olivary nucleus	0.48	0.06	<	0.50	0.05	0.036	0.04071
central medial thalamic nucleus	0.52	0.05	<	0.54	0.06	0.017	0.0384
Ventricle	0.52	0.06	<	0.54	0.06	0.029	0.04214
reticular nucleus	0.48	0.07	<	0.50	0.05	0.033	0.04473
lateral preoptic area	0.52	0.05	<	0.53	0.04	0.001	0.03037
tegmental nucleus	0.50	0.05	<	0.52	0.07	0.011	0.03654
CA3	0.49	0.04	<	0.50	0.04	0.024	0.02462
lateral amygdaloid nucleus	0.50	0.04	<	0.51	0.07	0.028	0.03662
nucleus lateral olfactory tract	0.46	0.04	<	0.47	0.06	0.047	0.02991
medial dorsal thalamic nucleus	0.48	0.04	<	0.48	0.06	0.040	0.0247
subiculum	0.53	0.05	<	0.54	0.04	0.014	0.01905
8th cerebellar lobule	0.49	0.05	<	0.50	0.06	0.029	0.02393
CA1	0.48	0.03	<	0.49	0.06	0.042	0.0192
lateral septal nucleus	0.52	0.08	<	0.53	0.07	0.011	0.02664
accumbens shell	0.51	0.06	<	0.52	0.06	0.012	0.02132

entorhinal ctx	**0.45**	**0.05**	**<**	**0.46**	**0.07**	**0.017**	***0.02447***
paraflocculus cerebellum	**0.50**	**0.03**	**>**	**0.49**	**0.07**	**0.047**	***0.01945***
extended amydala	**0.53**	**0.05**	**<**	**0.54**	**0.04**	**0.003**	***0.01581***
inferior colliculus	**0.47**	**0.04**	**<**	**0.47**	**0.07**	**0.008**	***0.02053***
endopiriform nucleus	**0.44**	**0.05**	**<**	**0.44**	**0.07**	**0.041**	***0.02301***
visual 2 ctx	**0.53**	**0.08**	**<**	**0.54**	**0.06**	**0.045**	***0.01821***
substantia nigra	**0.52**	**0.06**	**<**	**0.52**	**0.05**	**0.010**	***0.01221***
central amygdaloid nucleus	**0.45**	**0.04**	**<**	**0.45**	**0.06**	**0.037**	***0.01297***
olfactory tubercles	**0.49**	**0.08**	**<**	**0.50**	**0.07**	**0.034**	***0.01172***
retrosplenial ctx	**0.50**	**0.03**	**>**	**0.50**	**0.06**	**0.024**	***0.00761***
7th cerebellar lobule	**0.49**	**0.06**	**<**	**0.50**	**0.06**	**0.046**	***0.00868***
lateral hypothalamus	**0.45**	**0.05**	**<**	**0.45**	**0.07**	**0.033**	***0.00705***
diagonal band of Broca	**0.50**	**0.04**	**<**	**0.50**	**0.05**	**0.007**	***0.00393***
mammillary nucleus	**0.46**	**0.05**	**<**	**0.46**	**0.07**	**0.028**	***0.00318***

Fractional Anisotropy: Control Females and Males							
Brain Area	Females (n=17)			Males (n=19)			
	Mean	SD		Mean	SD	P val	Effect
parafascicular thalamic nucleus	0.48	0.06	>	0.39	0.07	0.000	0.32447
habenula nucleus	0.49	0.07	>	0.41	0.08	0.001	0.29116
lateral geniculate	0.56	0.05	>	0.47	0.07	0.000	0.26107
bed nucleus stria terminalis	0.48	0.04	>	0.41	0.05	0.000	0.26013
diagonal band of Broca	0.48	0.04	>	0.40	0.08	0.002	0.24076
claustrum	0.47	0.06	>	0.40	0.06	0.003	0.2303
lateral dorsal thalamic nucleus	0.58	0.05	>	0.51	0.10	0.005	0.21017
glomerular layer olfactory bulb	0.48	0.03	>	0.42	0.07	0.002	0.19975
lateral amygdaloid nucleus	0.50	0.08	>	0.43	0.08	0.020	0.19807
granular cell layer olfactory bulb	0.46	0.04	>	0.40	0.07	0.004	0.197
central medial thalamic nucleus	0.51	0.06	>	0.44	0.08	0.010	0.19131
pretectal nucleus	0.48	0.04	>	0.42	0.06	0.001	0.19005
ventral tegmental area	0.57	0.06	>	0.50	0.07	0.003	0.18642
anterior olfactory nucleus	0.48	0.03	>	0.42	0.06	0.001	0.1821
medial geniculate	0.52	0.04	>	0.46	0.08	0.005	0.18048
olfactory tubercles	0.52	0.03	>	0.46	0.07	0.002	0.17889
6th cerebellar lobule	0.48	0.05	>	0.42	0.06	0.003	0.178
medial preoptic area	0.51	0.03	>	0.45	0.08	0.006	0.17754
caudate putamen (striatum)	0.47	0.05	>	0.41	0.06	0.008	0.17608
posterior hypothalamic area	0.54	0.07	>	0.48	0.05	0.005	0.17523
orbital ctx	0.45	0.04	>	0.40	0.06	0.006	0.17508
tegmental nucleus	0.55	0.08	>	0.49	0.07	0.017	0.17139
reuniens nucleus	0.54	0.06	>	0.48	0.07	0.008	0.17084
dorsal raphe	0.52	0.07	>	0.46	0.08	0.024	0.17039
tenia tecta ctx	0.51	0.03	>	0.45	0.07	0.005	0.17023
red nucleus	0.53	0.06	>	0.47	0.07	0.010	0.16899
medial septum	0.48	0.07	>	0.43	0.07	0.035	0.16893
CA1	0.51	0.04	>	0.45	0.06	0.003	0.16838
posterior thalamic nucleus	0.52	0.03	>	0.46	0.07	0.004	0.16653
anterior thalamic nuclei	0.45	0.05	>	0.40	0.06	0.013	0.16469
substantia nigra	0.60	0.05	>	0.53	0.06	0.002	0.16259
secondary somaotsensory ctx	0.45	0.05	>	0.40	0.07	0.027	0.15839
lateral posterior thalamic nucleus	0.51	0.06	>	0.45	0.07	0.025	0.15525
CA3	0.53	0.04	>	0.47	0.07	0.007	0.15272
reticular formation	0.52	0.05	>	0.47	0.06	0.012	0.15052
dorsal medial nucleus	0.53	0.06	>	0.48	0.07	0.020	0.14557
accumbens core	0.53	0.04	>	0.48	0.06	0.003	0.14454
subiculum	0.49	0.04	>	0.45	0.06	0.011	0.13942
dentate gyrus	0.49	0.04	>	0.45	0.07	0.015	0.13789
ventral pallidum	0.53	0.04	>	0.48	0.06	0.008	0.13773
superior colliculus	0.44	0.04	>	0.40	0.06	0.019	0.13266

lateral preoptic area	0.56	0.04	>	0.51	0.08	0.023	0.1326
extended amydala	0.52	0.06	>	0.47	0.06	0.020	0.13195
parasubiculum	0.44	0.04	>	0.40	0.07	0.037	0.13104
median raphe nucleus	0.59	0.05	>	0.54	0.08	0.026	0.13094
interpeduncular nucleus	0.54	0.05	>	0.50	0.05	0.011	0.13013
7th cerebellar lobule	0.52	0.05	>	0.47	0.06	0.022	0.13013
accumbens shell	0.52	0.05	>	0.48	0.06	0.018	0.12372
zona incerta	0.64	0.05	>	0.58	0.07	0.018	0.11986
central amygdaloid nucleus	0.53	0.06	>	0.49	0.07	0.049	0.11951
8th cerebellar lobule	0.53	0.05	>	0.49	0.05	0.018	0.11938
endopiriform nucleus	0.49	0.06	>	0.45	0.05	0.046	0.11912
parabrachial nucleus	0.54	0.05	>	0.50	0.06	0.024	0.1173
paraventricular nuclus	0.55	0.06	>	0.50	0.07	0.040	0.11618
basal amygdaloid nucleus	0.56	0.05	>	0.51	0.07	0.046	0.11537
ventral thalamic nuclei	0.55	0.04	>	0.51	0.06	0.020	0.1152
9th cerebellar lobule	0.53	0.06	>	0.49	0.05	0.040	0.10817
pontine reticular nucleus oral	0.55	0.05	>	0.51	0.06	0.027	0.1075
cortical amygdaloid nucleus	0.53	0.04	>	0.50	0.06	0.040	0.10125
trigeminal complex medulla	0.53	0.02	>	0.49	0.05	0.007	0.09908
reticulotegmental nucleus	0.55	0.05	>	0.51	0.05	0.041	0.09501
crus ansiform lobule	0.50	0.04	>	0.47	0.05	0.040	0.08962

Apparent Diffusion Coefficient: Control Females and Males							
Brain Area	Females			Males			
	Mean	SD		Mean	SD	P val	Effect
cuneate nucleus	1.27	0.11	<	1.48	0.29	0.008	0.1919
9th cerebellar lobule	1.31	0.15	<	1.52	0.28	0.009	0.18698
tegmental nucleus	1.29	0.15	<	1.49	0.16	0.000	0.18492
7th cerebellar lobule	1.13	0.09	<	1.29	0.28	0.025	0.17274
parafascicular thalamic nucleus	1.24	0.11	<	1.41	0.18	0.001	0.17138
central medial thalamic nucleus	1.22	0.09	<	1.40	0.18	0.001	0.17085
dentate gyrus	1.40	0.15	<	1.60	0.22	0.003	0.17017
red nucleus	1.26	0.14	<	1.44	0.19	0.003	0.16745
perirhinal ctx	1.34	0.15	<	1.52	0.24	0.009	0.16346
habenula nucleus	1.34	0.11	<	1.52	0.24	0.009	0.15647
central amygdaloid nucleus	1.32	0.11	<	1.49	0.18	0.002	0.1552
ventral tegmental area	1.45	0.23	<	1.64	0.30	0.045	0.15392
reticular nucleus	1.29	0.09	<	1.46	0.18	0.002	0.15359
caudate putamen (striatum)	1.23	0.09	<	1.39	0.18	0.002	0.15305
accumbens core	1.25	0.10	<	1.40	0.15	0.001	0.14924
posterior thalamic nucleus	1.24	0.11	<	1.39	0.17	0.004	0.14636
globus pallidus	1.22	0.10	<	1.37	0.17	0.004	0.14432
zona incerta	1.32	0.16	<	1.47	0.21	0.018	0.14322
lateral amygdaloid nucleus	1.40	0.14	<	1.56	0.20	0.008	0.14169
temporal ctx	1.30	0.13	<	1.45	0.21	0.016	0.14155
median raphe nucleus	1.33	0.16	<	1.48	0.21	0.019	0.13934
parabrachial nucleus	1.31	0.14	<	1.46	0.17	0.008	0.13793
medial geniculate	1.26	0.12	<	1.40	0.17	0.007	0.13656
basal amygdaloid nucleus	1.31	0.17	<	1.45	0.18	0.021	0.13487
pontine reticular nucleus oral	1.34	0.21	<	1.48	0.22	0.047	0.13411
pretectal nucleus	1.28	0.10	<	1.42	0.18	0.007	0.13291
reticular formation	1.33	0.14	<	1.47	0.19	0.015	0.13201
claustrum	1.23	0.11	<	1.36	0.17	0.009	0.13179
White Matter	1.37	0.11	<	1.51	0.20	0.011	0.13133
reuniens nucleus	1.28	0.13	<	1.42	0.18	0.015	0.1309
ventral thalamic nuclei	1.28	0.11	<	1.41	0.18	0.010	0.13063
subiculum	1.40	0.16	<	1.55	0.20	0.021	0.12898
dorsal raphe	1.35	0.14	<	1.49	0.20	0.020	0.12782
lateral septal nucleus	1.45	0.12	<	1.60	0.18	0.008	0.12336
auditory ctx	1.29	0.12	<	1.42	0.19	0.023	0.12044
periaqueductal gray	1.41	0.11	<	1.55	0.22	0.027	0.11978
lateral posterior thalamic nucleus	1.30	0.10	<	1.43	0.17	0.012	0.11941
CA3	1.39	0.13	<	1.53	0.21	0.028	0.11874
posterior hypothalamic area	1.32	0.17	<	1.44	0.18	0.039	0.1185
infralimbic ctx	1.48	0.16	<	1.62	0.18	0.018	0.1179
CA1	1.40	0.12	<	1.53	0.19	0.017	0.11749

bed nucleus stria terminalis	**1.30**	**0.13**	**<**	**1.43**	**0.17**	**0.019**	***0.11585***
orbital ctx	**1.36**	**0.14**	**<**	**1.48**	**0.21**	**0.046**	***0.11332***
solitary tract nucleus	**1.30**	**0.13**	**<**	**1.42**	**0.20**	**0.044**	***0.11314***
paraventricular nuclus	**1.37**	**0.15**	**<**	**1.49**	**0.16**	**0.022**	***0.11212***
medial septum	**1.34**	**0.14**	**<**	**1.46**	**0.14**	**0.022**	***0.10701***
lateral geniculate	**1.31**	**0.11**	**<**	**1.42**	**0.18**	**0.034**	***0.10652***
extended amydala	**1.33**	**0.15**	**<**	**1.44**	**0.17**	**0.043**	***0.10648***

Apparent Diffusion Coefficient: Control Males vs Oxytocin Males							
Brain Area	Males Control			Males Oxytocin			
	Mean	SD		Mean	SD	P val	Effect
periaqueductal gray	1.55	0.22	>	1.31	0.14	0.000	0.25266
tegmental nucleus	1.49	0.16	>	1.26	0.13	0.000	0.24327
vestibular nucleus	1.48	0.16	>	1.26	0.15	0.000	0.22849
dorsal raphe	1.49	0.20	>	1.28	0.14	0.000	0.22449
parafascicular thalamic nucleus	1.41	0.18	>	1.22	0.12	0.000	0.22109
reuniens nucleus	1.42	0.18	>	1.22	0.14	0.000	0.22122
paraventricular nuclus	1.49	0.16	>	1.29	0.13	0.000	0.21074
posterior thalamic nucleus	1.39	0.17	>	1.21	0.13	0.000	0.20552
superior colliculus	1.45	0.19	>	1.26	0.13	0.000	0.20326
ventral thalamic nuclei	1.41	0.18	>	1.23	0.14	0.000	0.19862
CA3	1.53	0.21	>	1.33	0.15	0.000	0.20163
central amygdaloid nucleus	1.49	0.18	>	1.31	0.14	0.000	0.19427
central medial thalamic nucleus	1.40	0.18	>	1.22	0.12	0.000	0.19809
lateral amygdaloid nucleus	1.56	0.20	>	1.39	0.13	0.000	0.17413
medial dorsal thalamic nucleus	1.40	0.19	>	1.22	0.14	0.000	0.20071
pretectal nucleus	1.42	0.18	>	1.25	0.12	0.000	0.18295
secondary somaotsensory ctx	1.42	0.17	>	1.27	0.13	0.000	0.16995
medial geniculate	1.40	0.17	>	1.24	0.14	0.000	0.18186
bed nucleus stria terminalis	1.43	0.17	>	1.26	0.13	0.000	0.18427
accumbens core	1.40	0.15	>	1.24	0.12	0.000	0.17873
CA1	1.53	0.19	>	1.36	0.15	0.000	0.17772
lateral dorsal thalamic nucleus	1.48	0.18	>	1.32	0.13	0.000	0.16654
parabrachial nucleus	1.46	0.17	>	1.30	0.16	0.000	0.16313
lateral posterior thalamic nucleus	1.43	0.17	>	1.26	0.14	0.000	0.17875
red nucleus	1.44	0.19	>	1.27	0.14	0.000	0.18789
primary somatosensory ctx	1.55	0.21	>	1.39	0.17	0.001	0.15046
reticular nucleus	1.46	0.18	>	1.29	0.13	0.001	0.17881
inferior colliculus	1.50	0.21	>	1.30	0.14	0.001	0.20488
habenula nucleus	1.52	0.24	>	1.35	0.19	0.001	0.16646
medial septum	1.46	0.14	>	1.29	0.13	0.001	0.17305
paraventricular nucleus	1.40	0.19	>	1.23	0.17	0.001	0.18977
White Matter	1.51	0.20	>	1.35	0.15	0.001	0.16027
lateral geniculate	1.42	0.18	>	1.25	0.13	0.001	0.17768
2nd cerebellar lobule	1.47	0.20	>	1.30	0.21	0.001	0.17439
caudate putamen (striatum)	1.39	0.18	>	1.23	0.12	0.001	0.16938
claustrum	1.36	0.17	>	1.21	0.11	0.001	0.16714
anterior thalamic nuclei	1.40	0.18	>	1.24	0.15	0.001	0.17436
median raphe nucleus	1.48	0.21	>	1.33	0.17	0.001	0.14888
reticular formation	1.47	0.19	>	1.31	0.19	0.001	0.16269
accumbens shell	1.43	0.16	>	1.26	0.14	0.002	0.18139
auditory ctx	1.42	0.19	>	1.27	0.16	0.002	0.1609

globus pallidus	1.37	0.17	>	1.21	0.14	0.002	0.17193
orbital ctx	1.48	0.21	>	1.31	0.14	0.003	0.17342
infralimbic ctx	1.62	0.18	>	1.44	0.16	0.003	0.16252
7th cerebellar lobule	1.29	0.28	>	1.08	0.18	0.003	0.26364
visual 1 ctx	1.50	0.25	>	1.34	0.19	0.003	0.15891
anterior olfactory nucleus	1.57	0.30	>	1.35	0.22	0.003	0.21393
10th cerebellar lobule	1.62	0.25	>	1.43	0.17	0.003	0.18096
dentate gyrus	1.60	0.22	>	1.41	0.19	0.003	0.18057
agranular insular ctx	1.45	0.17	>	1.30	0.23	0.004	0.1574
5th cerebellar lobule	1.25	0.24	>	1.07	0.19	0.004	0.22931
extended amydala	1.44	0.17	>	1.29	0.17	0.004	0.15247
3rd cerebellar lobule	1.30	0.22	>	1.13	0.21	0.004	0.20307
endopiriform nucleus	1.40	0.18	>	1.26	0.18	0.005	0.15393
6th cerebellar lobule	1.24	0.23	>	1.03	0.18	0.005	0.26201
parasubiculum	1.57	0.28	>	1.42	0.21	0.005	0.14979
subiculum	1.55	0.20	>	1.40	0.24	0.007	0.13718
frontal association ctx	1.58	0.24	>	1.43	0.19	0.008	0.15083
zona incerta	1.47	0.21	>	1.31	0.22	0.011	0.17364
temporal ctx	1.45	0.21	>	1.30	0.22	0.012	0.15813
lateral septal nucleus	1.60	0.18	>	1.48	0.12	0.012	0.10938
primary motor ctx	1.60	0.27	>	1.49	0.19	0.014	0.09447
visual 2 ctx	1.66	0.31	>	1.52	0.20	0.015	0.12248
ventral pallidum	1.47	0.18	>	1.32	0.18	0.015	0.15104
pontine reticular nucleus oral	1.48	0.22	>	1.36	0.27	0.016	0.12224
solitary tract nucleus	1.42	0.20	>	1.28	0.21	0.016	0.14862
retrosplenial ctx	1.77	0.33	>	1.64	0.22	0.016	0.10686
basal amygdaloid nucleus	1.45	0.18	>	1.30	0.23	0.022	0.16251
anterior hypothalamic area	1.55	0.23	>	1.39	0.27	0.023	0.1591
9th cerebellar lobule	1.52	0.28	>	1.33	0.19	0.024	0.18827
posterior hypothalamic area	1.44	0.18	>	1.28	0.16	0.024	0.17083
medial preoptic area	1.57	0.25	>	1.41	0.23	0.024	0.15719
diagonal band of Broca	1.53	0.22	>	1.40	0.21	0.025	0.13414
pontine reticular nucleus caudal	1.49	0.22	>	1.38	0.34	0.025	0.1033
perirhinal ctx	1.52	0.24	>	1.36	0.31	0.028	0.16618
anterior cingulate ctx	1.75	0.24	>	1.58	0.20	0.028	0.14404
crus ansiform lobule	1.36	0.24	>	1.23	0.23	0.029	0.1512
8th cerebellar lobule	1.38	0.29	>	1.23	0.24	0.034	0.1625
gigantocellular reticular nucleus	1.53	0.26	>	1.43	0.38	0.036	0.10108
granular cell layer olfactory bulb	1.56	0.30	>	1.40	0.16	0.040	0.16061
cuneate nucleus	1.48	0.29	>	1.34	0.25	0.042	0.14091
dorsal medial nucleus	1.64	0.25	>	1.51	0.20	0.046	0.11454
medial amygdaloid nucleus	1.68	0.25	>	1.52	0.34	0.049	0.13551